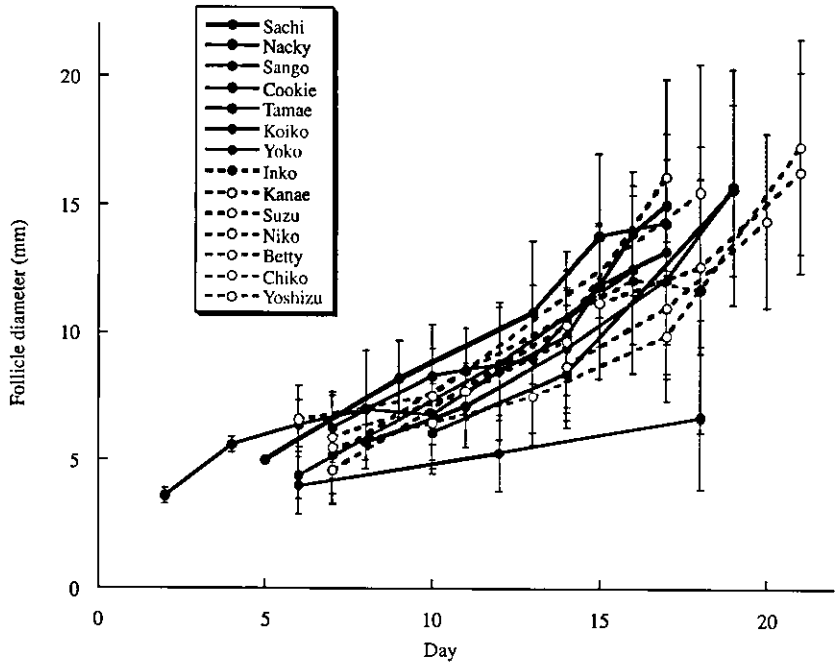

Fig. 3. Mean diameter of ovarian follicles measured by transvaginal ultrasonography in female chimpanzees treated with leuprorelin acetate plus human menopausal gonadotropin. Vertical bars represent standard deviations.

Follicle count

Time course changes in the follicle count measured by transvaginal ultrasonography are shown in Fig. 4A,B. The administration of leuprorelin acetate plus hMG increased the number of developing follicles, and the follicle count reached >30 in two subjects (Suzu and Chiko), 20–29 in six subjects (Cookie, Koiko, Yoko, Inko, Betty and Yoshizu), 10–19 in five subjects (Sachi, Sango, Tamae and Kanae) and <10 in one subject (Niko). However, four subjects, Sachi, Inko, Kanae and Betty, had subsequently lost >5 follicles by the final examination. The decrease in follicle count started at various time points (Fig. 4B).

Serum E_2 and P concentrations

Time course changes in serum E_2 concentrations are presented in Figs 5A,B and 6. There were great differences among the subjects. The peak E_2 concentration was >4000 pg/ml in three subjects (Nacky, Betty and Yoshizu), 2000–3000 pg/ml in three subjects (Cookie, Yoko and Suzu), 1000–2000 pg/ml in four subjects (Sango, Tamae, Kanae and Chiko) and <1000 pg/ml in four subjects (Sachi, Koiko, Inko and Niko). The E_2 concentration decreased rapidly after hCG administration in most of the subjects, but the decline started during hMG administration in Inko.

Time course changes in serum P concentrations are presented in Fig. 5A,B. The concentration was maintained at a very low level during hMG administration and rapidly increased after hCG administration. At oocyte retrieval, the serum P concentration reached >100 ng/ml in one subject (Nacky), 50–100 ng/ml in two subjects (Chiko and Yoshizu) and <50 ng/ml in 10 subjects (Sachi, Sango, Cookie, Tamae, Yoko, Inko, Kanae, Suzu, Niko and Betty).

Oocyte retrieval

Numbers and stages of oocytes retrieved are presented in Table 3. Five oocytes or more were retrieved from the aspirate of follicular fluid in nine subjects. In particular, >10 oocytes were obtained from Tamae, Betty and Chiko. In Inko and Kanae, COCs were collected from the aspirate of follicular fluid, but they did not contain any oocytes. Sachi and Niko possessed only a few or no follicles in the ovaries at the time of oocyte retrieval (35.5 h after hCG administration), respectively. In Sachi, only one oocyte was obtained from the aspirate of follicular fluid, and two oocytes were obtained from the aspirate of ascites in the pouch of Douglas. In Niko, ascites in the pouch of Douglas was aspirated, but no COCs were collected.

Most oocytes retrieved (92%) already had a first polar body and were estimated to be at the

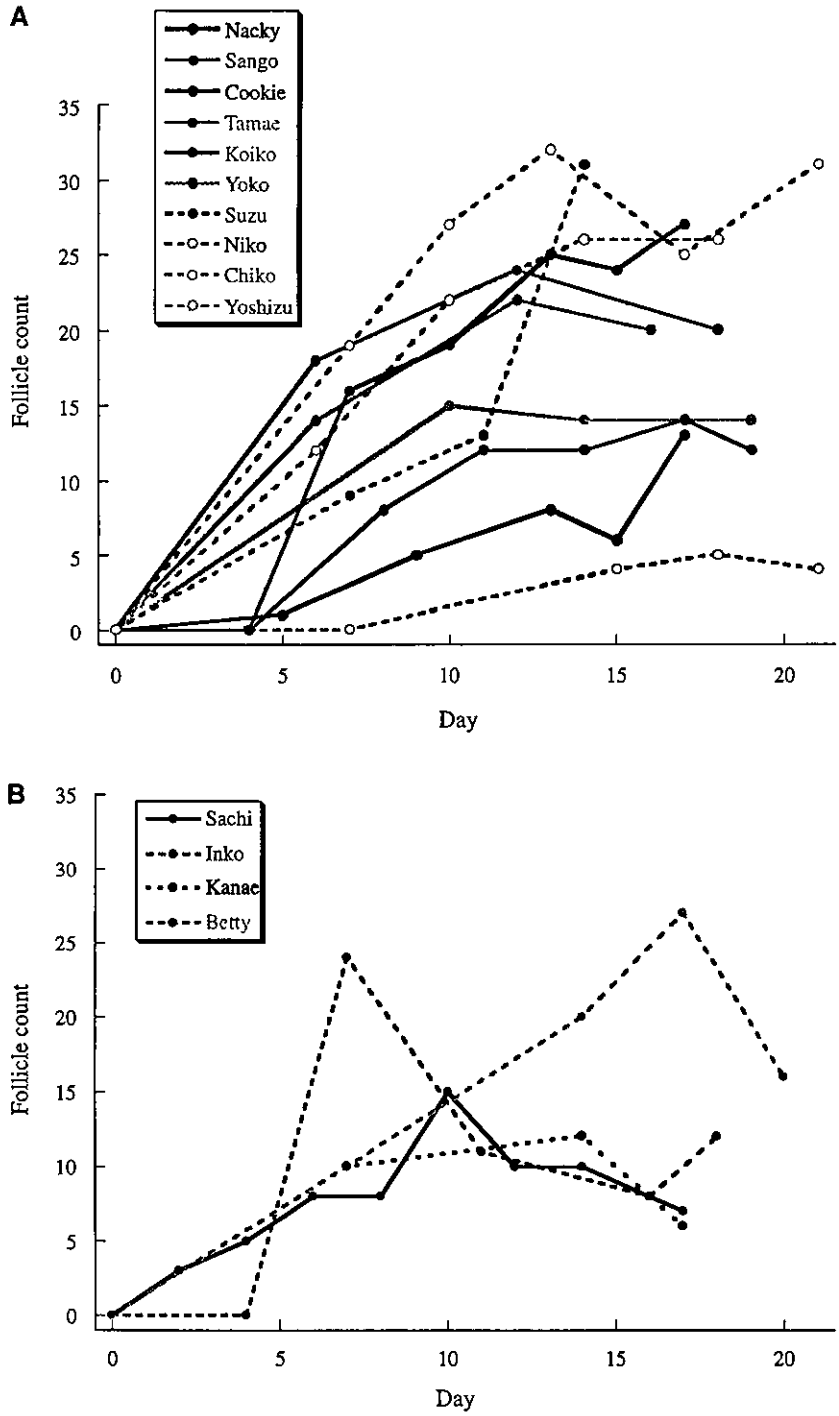

Fig. 4. Ovarian follicle counts measured by transvaginal ultrasonography in female chimpanzees treated with leuprorelin acetate plus human menopausal gonadotropin. Subjects who lost <5 follicles (A) or ≥5 follicles (B) during the dosing period.

metaphase II (M II) stage. Four oocytes (5%) did not have a polar body and were estimated to be at the stage of germinal vesicle breakdown (GVBD) or metaphase I (M I). Fragmentation was noted in only two oocytes (3%).

Statistical analysis on follicle development

The final follicle diameter was significantly dependent on the dosing duration and $\Sigma hMG_{D13\text{-final}}$ ($P < 0.05$; correlation coefficient = 0.546 and

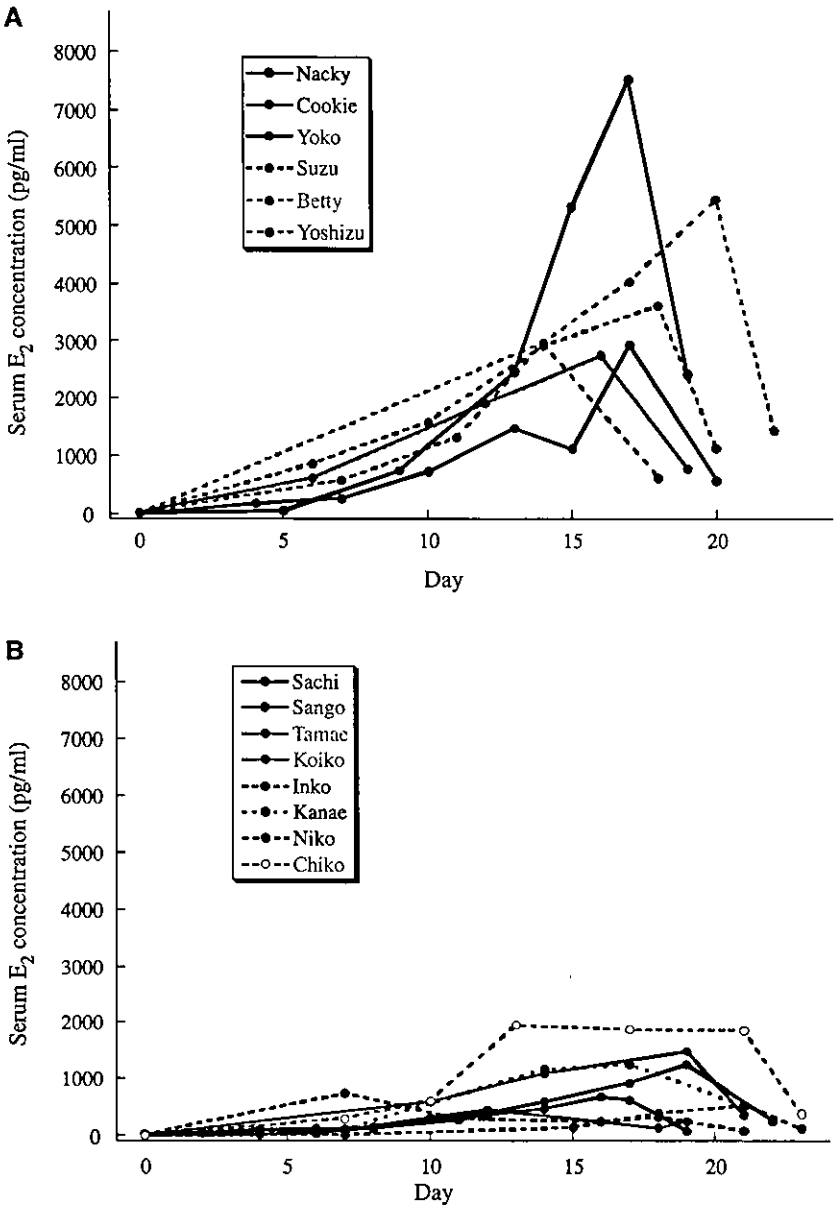

Fig. 5. Serum estradiol (E_2) concentrations in female chimpanzees stimulated with leuprorelin acetate plus human menopausal gonadotropin, followed by human chorionic gonadotropin. Subjects in which the maximum E_2 concentration reached ≥2000 pg/ml (A) or <2000 pg/ml (B) during the dosing period.

0.588, respectively), but not on age, $\Sigma hMG_{D1\text{-}final}$, $\Sigma hMG_{D1\text{-}6}$ or $\Sigma hMG_{D7\text{-}12}$ (Table 4). The maximum follicle count was significantly dependent on age and $\Sigma hMG_{D1\text{-}6}$ ($P < 0.05$; correlation coefficient = −0.561 and 0.567, respectively), but not on the dosing duration, $\Sigma hMG_{D1\text{-}final}$, $\Sigma hMG_{D7\text{-}12}$ or $\Sigma hMG_{D13\text{-}final}$ (Table 5). The decreased follicle count, which was defined as the difference between the maximum follicle count and the final follicle count, was not dependent on age, the dosing duration or any ΣhMG (Table 6).

OHSS-like symptoms

Five subjects (Nacky, Cookie, Yoko, Suzu and Betty) showed very mild OHSS-like symptoms, despite careful determination of the hMG regimen. At oocyte retrieval, they showed apparent ascites in the pouch of Douglas (Fig. 7). In 5 days, a decrease in food intake and sometimes in locomotion was observed. These signs disappeared within 2 weeks, and no abnormality was seen thereafter.

Endocrinologically, the mean peak E_2 concentration of these subjects was 4314 pg/ml, which was

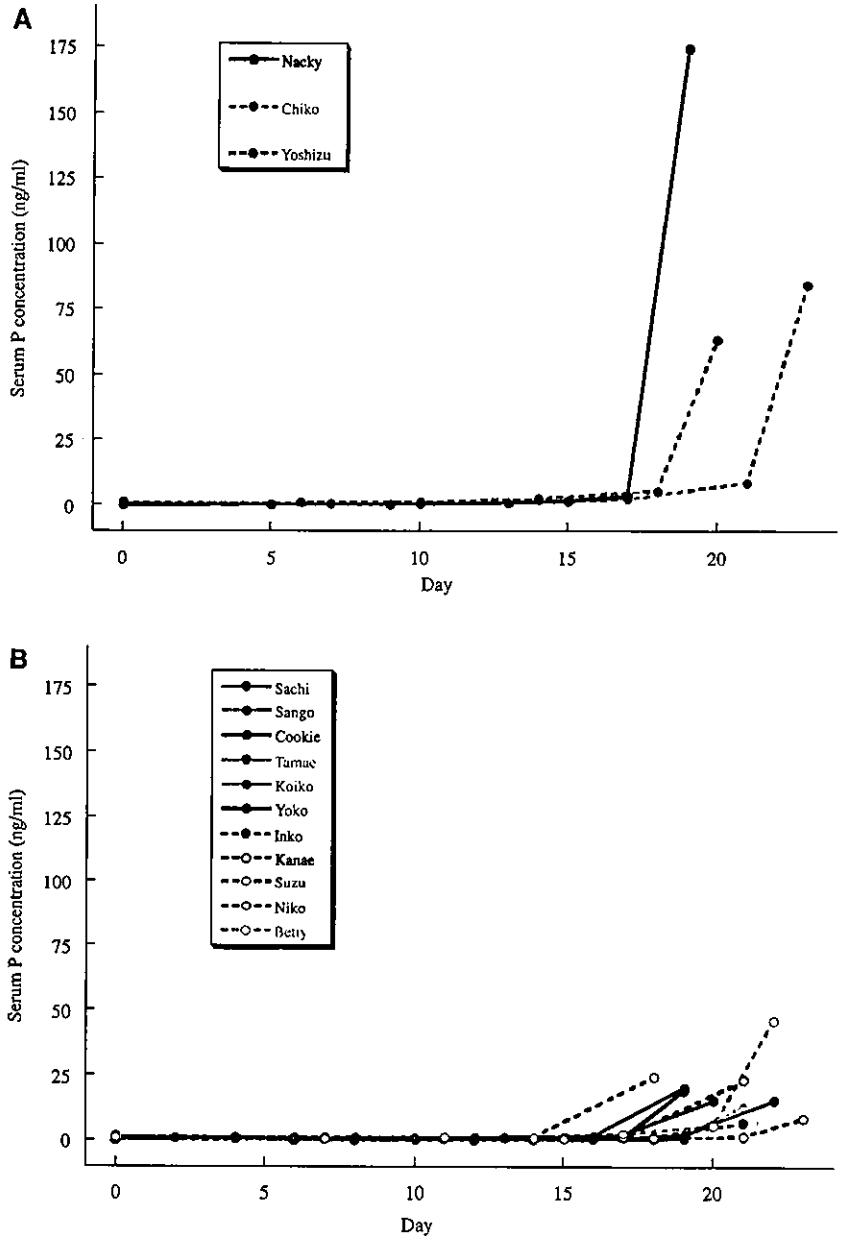

Fig. 6. Serum progesterone (P) concentrations in female chimpanzees stimulated with leuprorelin acetate plus human menopausal gonadotropin, followed by human chorionic gonadotropin. Subjects in which the P concentration at oocyte retrieval reached ≥50 pg/ml (A) or <50 pg/ml (B) during the dosing period.

significantly higher than that of the subjects apparently in normal health ($P < 0.05$). In contrast, there were no significant differences in the final follicle count or serum P concentration at oocyte retrieval between the two groups (Table 7).

Discussion

In the present study, we attempted ovarian stimulation with leuprorelin acetate plus hMG in 14 female chimpanzees and successfully induced the development of multiple follicles. The mean follicle diameter reached >10 mm at the final ultrasonographic examination in most of the subjects. The maximum follicle count during hMG administration was >30 in two subjects, 20–29 in six subjects, 10–19 in five subjects and <10 in one subject. Statistical analysis revealed the effect of the hMG regimen on follicular development. The final follicle diameter was dependent on the dosing duration and $\sum hMG_{D13\text{-final}}$, while the maximum follicle count was dependent on $\sum hMG_{D1\text{-}6}$. This

Table 3. Numbers and stages of oocytes retrieved in female chimpanzees stimulated with leuprorelin acetate plus human menopausal gonadotropin, followed by human chorionic gonadotropin (hCG)

Subject	Retrieval time (h)[1]	Number of oocytes	Stage		
			M II	GVBD – M I	Fragmented
Sachi	35.5	3[2]	3	0	0
Nacky	31	5	4	0	1
Sango	31	4	4	0	0
Cookie	30.5	5	4	0	1
Tamae	30	10	10	0	0
Koiko[3]	–	–	–	–	–
Yoko	30.5	9	9	0	0
Inko	30.5	0	–	–	–
Kanae	30	0	–	–	–
Suzu	33	5	4	1	0
Niko	35.5	0	–	–	–
Betty	30	16	16	0	0
Chiko	30	10	9	1	0
Yoshizu	30	8	6	2	0

GVBD, germinal vesicle breakdown; M I, metaphase I; M II, metaphase II.
[1]Time after hCG administration.
[2]Two oocytes were collected from ascites in the pouch of Douglas.
[3]Oocyte retrieval was not performed due to low food-intake and oliguria.

Table 4. Correlation coefficient and univariate linear regression analysis of the final follicle diameter (mm) in female chimpanzees stimulated with leuprorelin acetate plus human menopausal gonadotropin (hMG)

Factor	Correlation coefficient	Univariate linear regression analysis	
		r^1	*P*-value
Age (year)	0.156	0.064	0.595
Dosing duration (day)	0.546	0.794	0.043*
$\sum hMG_{D1\text{-}final}$ (IU day/kg)[2]	0.424	0.033	0.646
$\sum hMG_{D1\text{-}D6}$ (IU day/kg)[3]	−0.145	−0.062	0.621
$\sum hMG_{D7\text{-}D12}$ (IU day/kg)[4]	0.304	0.104	0.291
$\sum hMG_{D13\text{-}final}$ (IU day/kg)[5]	0.588	0.120	0.027*

[1]Regression coefficient.
[2]Total hMG dose per body weight from day 1 to the final ultrasonographic examination.
[3]Total hMG dose per body weight from day 1 to day 6.
[4]Total hMG dose per body weight from day 7 to day 12.
[5]Total hMG dose per body weight from day 13 to the final ultrasonographic examination.
*Significant *P*-values ($P < 0.05$).
The day of leuprorelin acetate administration was designated day 0.

analysis suggests that sufficient exposure to hMG in the early stage is needed to increase the number of developing follicles and that sufficient and continuous exposure to hMG in the late stage is needed to increase the size of growing follicles. In addition, the maximum follicle count was conversely correlated

Table 5. Correlation coefficient and univariate linear regression analysis of the maximum follicle count in female chimpanzees stimulated with leuprorelin acetate plus human menopausal gonadotropin (hMG)

Factor	Correlation coefficient	Univariate linear regression analysis	
		r^1	*P*-value
Age (year)	−0.561	−0.655	0.037*
Dosing duration (day)	−0.223	−0.913	0.444
$\sum hMG_{D1\text{-}final}$ (IU day/kg)[2]	0.097	0.034	0.743
$\sum hMG_{D1\text{-}D6}$ (IU day/kg)[3]	0.567	0.683	0.034*
$\sum hMG_{D7\text{-}D12}$ (IU day/kg)[4]	−0.036	−0.035	0.902
$\sum hMG_{D13\text{-}final}$ (IU day/kg)[5]	−0.097	−0.058	0.741

[1]Regression coefficient.
[2]Total hMG dose per body weight from day 1 to the final ultrasonographic examination.
[3]Total hMG dose per body weight from day 1 to day 6.
[4]Total hMG dose per body weight from day 7 to day 12.
[5]Total hMG dose per body weight from day 13 to the final ultrasonographic examination.
*Significant *P*-values ($P < 0.05$).
The day of leuprorelin acetate administration was designated day 0.

Table 6. Correlation coefficient and univariate linear regression analysis of the decreased follicle count in female chimpanzees stimulated with leuprorelin acetate plus human menopausal gonadotropin (hMG)

Factor	Correlation coefficient	Univariate linear regression analysis	
		r^1	*P*-value
Age (year)	0.109	0.064	0.711
Dosing duration (day)	−0.096	0.199	0.744
$\sum hMG_{D1\text{-}final}$ (IU day/kg)[2]	−0.134	−0.024	0.649
$\sum hMG_{D1\text{-}D6}$ (IU day/kg)[3]	0.144	0.088	0.624
$\sum hMG_{D7\text{-}D12}$ (IU day/kg)[4]	−0.271	−0.133	0.348
$\sum hMG_{D13\text{-}final}$ (IU day/kg)[5]	−0.128	−0.039	0.663

[1]Regression coefficient.
[2]Total hMG dose per body weight from day 1 to the final ultrasonographic examination.
[3]Total hMG dose per body weight from day 1 to day 6.
[4]Total hMG dose per body weight from day 7 to day 12.
[5]Total hMG dose per body weight from day 13 to the final ultrasonographic examination.
The decreased follicle count was defined as the difference between the maximum follicle count and the final follicle count.
The day of leuprorelin acetate administration was designated day 0.

with age. In contrast, the decreased follicle count was independent of age, dosing duration or any $\sum$hMG.

It has been reported that a single administration of hMG or follicle stimulating hormone (FSH) in the early follicular phase increases the number of small follicles and stimulates proliferation of granulosa cells in humans [12, 36], suggesting that

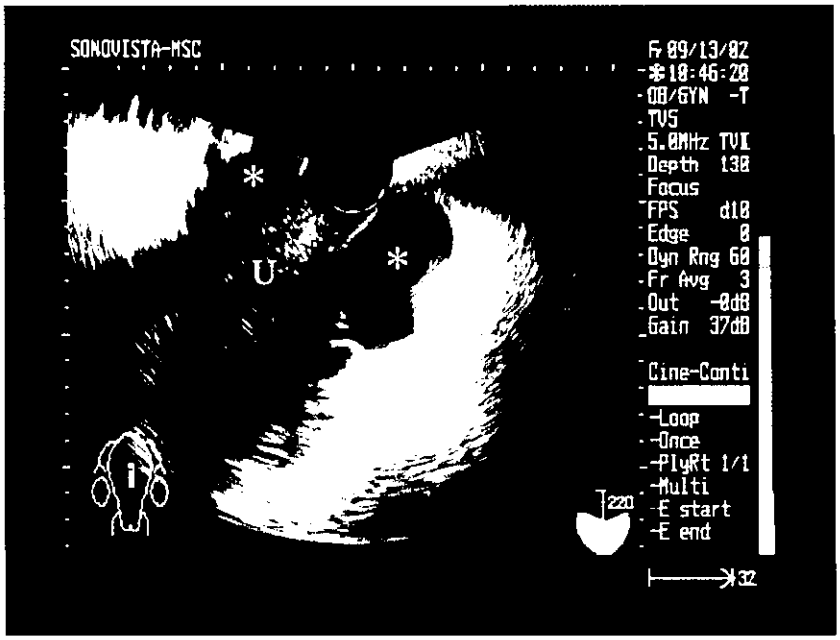

Fig. 7. A transvaginal ultrasonograph at oocyte retrieval in a subject showing OHSS-like symptoms (Nacky). Asterisks indicate ascites in the pouch of Douglas. U indicates the uterus.

Table 7. The final follicle count, serum peak estradiol (E_2) concentration during hMG administration and serum progesterone (P) concentration at oocyte retrieval in female chimpanzees apparently in normal health and those showing ovarian hyperstimulation syndrome (OHSS)-like symptoms

Group	Normal[1]	OHSS-like[2]
n	9	5
Final follicle count	15 ± 11	21 ± 8
Peak E_2 (pg/mL)[3]	1323 ± 988	4314 ± 2114*
P (pg/mL) at oocyte retrieval	29.0 ± 28.5	40.7 ± 54.9

[1]Subjects apparently in normal health.
[2]Subjects showing OHSS-like symptoms (see text for details).
[3]Peak concentration during the dosing period.
*Significantly different from the normal group with Aspin-Welch's test ($P < 0.05$).
Values shown are mean values ± SD.

a short, but distinct, increase in the hMG or FSH level can accelerate follicle recruitment in the early follicular phase. Therefore, the dependency of the maximum follicle count on $\Sigma hMG_{D1\text{-}6}$ in the present study may indicate that the increased hMG exposure in the early stage accelerates follicle recruitment also in chimpanzees.

In addition, a converse correlationship between the maximum follicle count and age was detected in the present study. It has been reported that the number of growing follicles reflects the total number of follicles present in the ovary, which is the major factor determining the response to exogenous gonadotropins [4]. Therefore, this result might reflect the decrease in the total number of follicles with age in chimpanzees.

In contrast to early follicle development, advanced follicle development requires continuous stimulation by gonadotropins. In the normal menstrual cycle, the FSH concentration reaches a maximum in the early follicular phase. Maturating follicles secrete estrogens and inhibins, which suppress pituitary FSH release via a feedback mechanism. The maturing follicles are very sensitive to FSH, and they can keep growing after pituitary FSH suppression. In contrast, the other immature follicles cannot avoid undergoing atresia [3, 21]. Exogenous gonadotropin treatment in the mid- to late follicular phase compensates for the endogenous pituitary FSH suppression and rescues immature follicles from atresia [36]. Thus, the continuous hMG administration in the intermediate and late stages may have helped to maintain multiple follicle development until oocyte retrieval in the present study.

Despite continuous hMG administration, however, four subjects, Sachi, Inko, Kanae and Betty, lost >5 follicles, indicating that the follicles underwent atresia. The reason why follicle atresia occurred in these subjects is unclear. The decreased follicle count was not affected by age, dosing duration or any $\sum hMG$, and the decrease started at various time points. Further study will be needed to detect the factors responsible for atresia.

Recent studies have suggested that the follicle atresia can be explained, at least in part, by the apoptosis of granulosa cells [19, 40]. It has been reported that cell-death ligand and receptor systems, such as the Fas ligand and Fas system, the tumor necrosis factor (TNF)-α and TNF-receptor system, and the TNF-α-related apoptosis-inducing ligand (TRAIL) and TRAIL-receptor system, are involved in the regulatory mechanisms of granulosa cell apoptosis in mice and pigs [28, 33, 35, 41, 42]. Although there are species-specific differences in the apoptosis of granulosa cells [27], some cell-death ligand and receptor systems could be involved in the regulation of follicle atresia in chimpanzees.

The final diameter was statistically dependent on the dosing duration and $\sum hMG_{D13\text{-}final}$, despite no great inter-individual difference in the follicle growth rate. It has been reported that continuous exposure to FSH is needed for follicle maturation and that the fully matured follicle possesses high aromatase activity in granulosa cells. In addition, the amount of E_2 synthesed by granulosa cells is correlated with the size of large follicles [21]. Thus, prolonged and increased hMG exposure in the late stage might promote final follicle maturation, resulting in the increased final follicle diameter in the present study.

We obtained multiple oocytes from most of the subjects by ultrasound-guided transvaginal aspiration without significant adverse events. However, the oocyte retrieval was unsuccessful in certain subjects. In the cases of Sachi and Niko, a few follicles or less remained at the time of oocyte retrieval, indicating that ovulation had already occurred. In these subjects, the aspiration was performed at 35.5 h after hCG administration, which was later than in the others (30–33 h after hCG administration). This result indicates that oocyte retrieval should be performed within 33 h of the administration of hCG in chimpanzees. On the other hand, no oocyte was collected from Inko and Kanae, because the COCs collected from them did not contain any oocytes. Interestingly, these subjects showed relatively low serum E_2 levels and lost >5 follicles during hMG administration. It is speculated that the remaining follicles at oocyte retrieval were already atretic and that the oocytes were degenerative.

OHSS is an iatrogenic and potentially life-threatening complication of ovulatory stimulation. It has been reported that OHSS is associated with symptoms such as abdominal bloating, nausea, vomiting, enlarged ovaries, ascites, pleural and pericardial effusions, hemoconcentration, hypercoagulation and serum electrolyte imbalance [10, 26]. A high serum E_2 concentration and an increased number of follicles are among the risk factors for OHSS, and most studies in humans have selected 3000 pg/ml of E_2 as a safe value for hCG administration [1]. In the present study, five subjects showed apparent ascites with a decrease in food intake and locomotion, suggesting the occurrence of very mild OHSS. They showed a significantly higher peak serum E_2 concentration than the others, and their mean concentration (4314 pg/ml) was above the safe value for humans. This result suggests that the peak serum E_2 concentration was predictive of OHSS-like symptoms in chimpanzees. On the other hand, there was no significant difference in the final follicle count between the two groups, suggesting that the increased number of follicles was not an indicator of OHSS-like symptoms in chimpanzees.

Although a rise in the E_2 concentration precedes OHSS, E_2 itself is not a causal factor of this disease [24]. After hCG administration, matured follicles are ruptured and transformed to corpora lutea. During luteinization, a basket-like capillary wreath surrounding the follicular basement membrane is reconstructed to form a capillary network in the corpus luteum [5, 20, 38]. This drastic change in the microvasculature is accompanied by angiogenesis and capillary hyperpermeability, which is induced by vascular endothelial cell growth factor (VEGF) [9, 39, 43]. In mice, luteinization, neovascularization and edema simultaneously occur in theca interna before ovulation [38]. VEGF is also considered to be the primary molecule involved in the pathogenesis of OHSS, because capillary hyperpermeability is the major initial change leading to the full appearance and maintenance of this disease [2, 34, 43]. Thus the occurrence of OHSS is closely related with angiogenesis and capillary hyperpermeability during luteinization. However, there was no significant difference in serum P concentrations at oocyte retrieval between subjects in normal health and those showing OHSS-like symptoms in the present study. This contradiction might be explained by the notion that angiogenesis and capillary hyperpermeability before ovulation are independent of the secretion of P from luteinizing theca cells.

Although we statistically detected the dependence of follicular development on hMG dose, a great variation was noted in response to hMG. It has been reported that the response to exogenous FSH therapy is quite variable and associated with the polymorphism of ovarian FSH receptor in humans [23]. Therefore, the variation in response to hMG could be caused by the polymorphism of ovarian FSH receptor in the present study.

We succeeded in obtaining multiple oocytes from chimpanzees. Most of them were at the M II stage, suggesting that the dosing regimen of the present study was appropriate for oocyte maturation in follicles. However, further investigation will be needed for their application. It has been reported that a rise in the E_2 concentration after administration of hMG or leuprorelin acetate is predictive of IVF success in humans [8, 32]. Therefore, the relationship between the serum E_2 concentration and the potential of retrieved oocytes should be examined to optimize the procedure of hormone treatment. In addition, one should undertake the optimization for each subject, because there are great inter-individual differences in pituitary and ovarian hormone dynamics in chimpanzees.

In conclusion, we successfully stimulated ovaries with leuprorelin acetate plus hMG administration for multiple follicle development and multiple oocyte retrieval in chimpanzees. The present study also suggested that the dose of hMG affected the number of developing follicles in the early stage and follicle maturation in the late stage. In addition, the peak serum E_2 concentration was shown to be predictive of OHSS-like symptoms. The results of the present investigation should help to resolve various problems arising from the circumstances of this endangered species.

References

1. ABOULGHAR M: Prediction of ovarian hyperstimulation syndrome (OHSS): estradiol level has an important role in the prediction of OHSS. Hum Reprod 18:1140–1141, 2003.
2. ALBERT C, GARRIDO N, MERCADER A, RAO CV, REMOHÍ J, SIMÓN CA: The role of endothelial cells in the pathogenesis of ovarian hyperstimulation syndrome. Mol Hum Reprod 8:409–418, 2002.
3. BAIRD DT: A model for follicular selection and ovulation: lessons from superovulation. J Steroid Biochem 27:15–23, 1987.
4. BAIRD DT, PEARSON S: Factors determining response to controlled ovarian stimulation (COS) for in vitro fertilization (IVF). In: *Evidence-Based Fertility Treatment*. TEMPLETON, COOKE & O'BRIEN (eds). RCOG Press: London 274–282, 1998.
5. BASSETT DL: The changes in the vasculature pattern of the ovary of the albino rat during the estrous cycle. Am J Anat 73:251–291, 1943.
6. BUXHOEVEDEN DP, SWITALA AE, ROY E, LITAKER M, CASANOVA MF: Morphological differences between minicolumns in human and nonhuman primate cortex. Am J Phys Anthropol 115:361–371, 2001.
7. DUKELOW WR: Induction and timing of single and multiple ovulations in the squirrel monkey (*Saimiri sciureus*). J Reprod Fertil 22:303–309, 1970.
8. FABREGUES F, BALASCH J, CREUS M, CARMONA F, PUERTO B, QUINTO L, CASAMITJANA R, VANRELL JA: Ovarian reserve test with human menopausal gonadotropin as a predictor of in vitro fertilization outcome. J Assist Reprod Genet 17:13–19, 2000.
9. FRASER HM, WULFF C: Angiogenesis in the primate ovary. Reprod Fertil Dev 13:557–566, 2001.
10. GOLAN A, RON-EL R, HERMAN A, SOFFER Y, WANIRAUB Z, CAPSI E: Ovarian hyperstimulation syndrome. An update review. Obstet Gynaecol Surv 44:430–440, 1989.
11. GORBA T, ALLSOPP TE: Pharmacological potential of embryonic stem cells. Pharmacol Res 47:269–278, 2003.
12. GOUGEON A, TESTART J: Influence of human menopausal gonadotropin on the recruitment of human ovarian follicles. Fertil Steril 54:848–852, 1990.
13. GOUGEON A, LEFEVRE B, TESTART J: Influence of a gonadotropin-releasing hormone agonist and gonadotropins on morphometric characteristics of the population of small ovarian follicles in cynomolgus monkeys (*Macaca fascicularis*). J Reprod Fertil 95:567–575, 1992.
14. GOULD KG: Ovum recovery and in vitro fertilization in the chimpanzee. Fertil Steril 40:378–383, 1983.
15. HATASAKA HH, SCHAFFER NE, CHENETTE PE, KOWALSKI W, HECHT BR, MEEHAN TP, WENTZ AC, VALLE RF, CHATTERTON RT, JEYENDRAN RS: Strategies for ovulation induction and oocyte retrieval in the lowland gorilla. J Assist Reprod Genet 14:102–110, 1997.
16. HOBSON WC, GRAHAM CE, ROWELL TJ: National chimpanzee breeding program: primate research institute. Am J Primatol 24:257–263, 1991.
17. HOHMANN FP, LAVEN JS, DE JONG FH, EIJKEMANS MJ, FAUSER BCJM: Low-dose exogenous FSH during the early, mid or late follicular phase can induce multiple dominant follicle development. Hum Reprod 16:846–854, 2001.
18. HOULDSWORTH J, HEATH SC, BOSL GJ, STUDER L, CHAGANTI RSK: Expression profiling of lineage differentiation in pluripotential human embryonal carcinoma cells. Cell Growth Differ 13:257–264, 2002.
19. HUGHES FM, GOROSPE WC: Biochemical identification of apoptosis (programmed cell death) in granulosa cells: evidence for a potential mechanism underlying follicular atresia. Endocrinology 129:2415–2422, 1991.
20. KANZAKI H, OKAMURA H, OKUDA Y, TAKENAKA A, MORIMOTO K, NISHIMURA T: Scanning electron microscopic study of rabbit ovarian follicle microvasculature using resin injection-corrosion cast. J Anat 134:697–704, 1982.
21. MACKLON NS, FAUSER BCJM: Follicle-stimulating hormone and advanced follicle development in the human. Arch Med Res 32:595–600, 2001.
22. MARSHALL VS, BROWNE MA, KNOWLES L, GOLOS TG, THOMSON JA: Ovarian stimulation of marmoset monkeys (*Callithrix jacchus*) using recombinant human follicle stimulating hormone. J Med Primatol 32:57–66, 2003.
23. MAYORGA MP, GROMOLL J, BEHRE HM, GASSNER C, NIESCHLAG E, SIMONI M: Ovarian response to follicle-stimulating hormone (FSH) stimulation depends on the FSH receptor genotype. J Clin Endocrinol Metab 85:3365–3369, 2000.
24. MEIROW D, SCHENKER J, ROSLER A: Ovarian hyperstimulation syndrome with low estradiol non-classical 17 alpha hydroxylase, 17–20 lyase deficiency: what is the role of oestrogens? Hum Reprod 11:2119–2121, 1996.
25. MUCHMORE EA: Chimpanzee models for human disease and immunobiology. Immunol Rev 183:86–93, 2001.
26. NAVOT D, BERGH PA, LAUFER N: Ovarian hyperstimulation syndrome in novel reproductive technologies: prevention and treatment. Fertil Steril 58:249–261, 1992.

27. NAKAYAMA M, MANABE N, NISHIHARA S, MIYAMOTO H: Species-specific differences in apoptotic cell localization in granulosa and theca interna cells during follicular atresia in porcine and bovine ovaries. J Reprod Dev 46:147–156, 2000.
28. NAKAYAMA M, MANABE N, INOUE N, MATSUI T, MIYAMOTO H: Changes in the expression of tumor necrosis factor (TNF) α, TNFα receptor (TNFR) 2, and TNFR-associated factor 2 in granulosa cells during atresia in pig ovaries. Biol Reprod 68:530–535, 2003.
29. NIWA H: Molecular mechanism to maintain stem cell renewal of ES cells. Cell Struct Funct 26:137–148, 2001.
30. ODORICO JS, KAUFMAN DS, THOMSON JA: Multilineage differentiation from human embryonic stem cell lines. Stem Cells 19:193–204, 2001.
31. OLSON MV, VARKI A: Sequencing the chimpanzee genome: insights into human evolution and disease. Nat Rev Genet 4:20–28, 2003.
32. PADILLA SL, BAYATI J, GARCIA JE: Prognostic value of the early serum estradiol response to leuprolide acetate in in vitro fertilization. Fertil Steril 53:288–294, 1990.
33. PRANGE-KIEL J, KREUTZKAMM C, WEHRENBERG U, RUNE GM: Role of tumor necrosis factor in preovulatory follicles of swine. Biol Reprod 65:928–935, 2001.
34. REYNOLDS LP, GRAZUL-BILSKA AT, REDMER DA: Angiogenesis in the female reproductive organs: pathological implications. Int J Exp Pathol 83:151–163, 2002.
35. SAKAMAKI K, YOSHIDA H, NISHIMURA Y, NISHIKAWA S, MANABE N, YONEHARA S: Involvement of Fas antigen in ovarian follicular atresia and luteolysis. Mol Reprod Dev 47:11–18, 1997.
36. SCHIPPER I, HOP WCJ, FAUSER BCJM: The follicle-stimulating hormone (FSH) threshold/window concept examined by different interventions with exogenous FSH during the follicular phase of the normal menstrual cycle: duration, rather than magnitude, of FSH increase affects follicle development. J Clin Endocrinol Metab 83:1292–1298, 1998.
37. SHIMIZU K, DOUKE C, FUJITA S, MATSUZAWA T, TOMONAGA M, TANAKA M, MATSUBAYASHI K, HAYASHI M: Urinary steroids, FSH and CG measurements for monitoring the ovarian cycle and pregnancy in the chimpanzee. J Med Primatol 32:15–22, 2003.
38. SHIMODA K, SATO E, TANAKA T, TAKEYA T, TOYODA Y: Morphological differentiation of the microvasculature during follicular development, ovulation and luteinization of mouse ovaries. Dev Growth Differ 35:431–437, 1993.
39. STOUFFER RL, MARTINEZ-CHEQUER JC, MOLSKNESS TA, XU F, HAZZARD TM: Regulation and action of angiogenic factors in the primate ovary. Arch Med Res 32:567–575, 2001.
40. TILLY JL, KOWALSKI KI, JOHNSON AL, HSUEH JW: Involvement of apoptosis in ovarian follicular atresia and postovulatory regression. Endocrinology 129:2799–2801, 1991.
41. WADA S, MANABE N, INOUE N, NAKAYAMA M, MATSUI T, MIYAMOTO H: Trail-decoy receptor-1 disappears in granulosa cells of atretic follicles in porcine ovaries. J Reprod Dev 48:167–173, 2002.
42. WADA S, MANABE N, INOUE N, NAKAYAMA M, MATSUI T, MIYAMOTO H: TRADD is involved in apoptosis induction in granulosa cells during atresia in pig ovaries. J Reprod Dev 48:175–181, 2002.
43. WANG TH, HORNG SG, CHANG CL, WU HM, TSAI YJ, WANG HS, SOONG YK: Human chorionic gonadotropin-induced ovarian hyperstimulation syndrome is associated with up-regulation of vascular endothelial growth factor. J Clin Endocrinol Metab 87:3300–3308, 2002.
44. WOBUS AM: Potential of embryonic stem cells. Mol Aspects Med 22:149–164, 2001.
45. YANO J, NODA Y, IDA K, MORI T, GOULD KG: In vitro fertilization and embryo transfer in the chimpanzee. Jpn J Fertil Streril 33:169–173, 1988 [in Japanese].
46. ZELINSKI-WOOTEN MB, HUTCHISON JS, HESS DL, WOLF DP, STOUFFER RL: Follicle stimulating hormone alone supports follicle growth and oocyte development in gonadotropin-releasing hormone antagonist-treated monkeys. Hum Reprod 10:1658–1666, 1995.

Early-Onset Macular Degeneration with Drusen in a Cynomolgus Monkey (*Macaca fascicularis*) Pedigree: Exclusion of 13 Candidate Genes and Loci

Shinsuke Umeda,[1,2] *Radha Ayyagari,*[3] *Rando Allikmets,*[4] *Michihiro T. Suzuki,*[5] *Athancios J. Karoukis,*[3] *Rajesh Ambasudhan,*[3] *Jana Zernant,*[4] *Haru Okamoto,*[1] *Fumiko Ono,*[5] *Keiji Terao,*[6] *Atsushi Mizota,*[7] *Yasuhiro Yoshikawa,*[2] *Yasuhiko Tanaka,*[1] *and Takeshi Iwata*[1]

Purpose. To describe hereditary macular degeneration observed in the cynomolgus monkey (*Macaca fascicularis*), which shares phenotypic features with age-related macular degeneration in humans, and to test the involvement of candidate gene loci by mutation screening and linkage analysis.

Methods. Ophthalmic examinations with fundus photography, fluorescein angiography (FA), indocyanine green angiography (IA), electroretinography (ERG), and histologic studies were performed on both affected and unaffected monkeys in the pedigree. The monkey orthologues of the human *ABCA4*, *VMD2*, *EFEMP1*, *TIMP3*, and *ELOVL4* genes were cloned and screened for mutations by single-strand conformation polymorphism (SSCP) analysis or denaturing high-performance liquid chromatography (DHPLC) and direct sequencing in six affected and five unaffected monkeys from the pedigree and in six unrelated, unaffected monkeys. Subsequently, 13 human macular degeneration loci including these five genes were analyzed to test for linkage with the disease. Nineteen affected and seven unaffected monkeys in the pedigree were analyzed by using human microsatellite markers linked to the 13 loci.

Results. Yellowish white spots were observed in the macula and fovea centralis, and in some cases the spots scattered to the peripheral retina along the blood vessels. FA showed hyperfluorescence corresponding to the dots except in the foveola. No anomalies were found by IA and ERG. Histologic studies demonstrated that the spots were drusen. Mutation analysis of the *ABCA4*, *VMD2*, *EFEMP1*, *TIMP3*, and *ELOVL4* genes identified a few sequence variants, but none of them segregated with the disease. Linkage analysis with markers linked to these five genes and an additional eight human macular degeneration loci failed to establish linkage. Haplotype analysis excluded the involvement of the 13 candidate loci for harboring the gene associated with macular degeneration in the monkeys.

Conclusions. Significant homology was identified between monkey and human orthologues of the five macular degeneration genes. Thirteen loci associated with macular degeneration in humans or harboring macular degeneration genes were excluded as causal of early-onset macular degeneration in the monkeys. It is likely that none of these loci, but rather a novel gene, is involved in causing the observed phenotype in this monkey pedigree. (*Invest Ophthalmol Vis Sci.* 2005;46:683–691) DOI:10.1167/iovs.04-1031

From the [1]National Institute of Sensory Organs, National Hospital Organization Tokyo Medical Center, Tokyo, Japan; the [2]Department of Biomedical Science, Graduate School of Agricultural and Life Sciences, The University of Tokyo, Tokyo, Japan; the [3]Department of Ophthalmology, Kellogg Eye Center, University of Michigan, Ann Arbor, Michigan; the [4]Departments of Ophthalmology and Pathology, Columbia University, New York, New York; The [5]Corporation for Production and Research of Laboratory Primates, Ibaraki, Japan; the [6]Tsukuba Primate Center for Medical Science, National Institute of Infectious Diseases, Ibaraki, Japan; and the [7]Department of Ophthalmology, Juntendo University Urayasu Hospital, Chiba, Japan.

Supported by research grant, Research on Measures for Intractable Diseases, Ministry of Health, Labor and Welfare of Japan and by the fellowship of the Promotion of Science for Japanese Junior Scientists (SU); The Foundation Fighting Blindness (RAl, RAy), National Eye Institute Grants EY13435 (RAl) and EY13198 (RAy), Research to Prevent Blindness (RAl, RAy) and Core Grant EY07003.

Submitted for publication August 27, 2004; revised November 1, 2004; accepted November 5, 2004.

Disclosure: **S. Umeda**, None; **R. Ayyagari**, None; **R. Allikmets**, None; **M.T. Suzuki**, None; **A.J. Karoukis**, None; **R. Ambasudhan**, None; **J. Zernant**, None; **H. Okamoto**, None; **F. Ono**, None; **K. Terao**, None; **A. Mizota**, None; **Y. Yoshikawa**, None; **Y. Tanaka**, None; **T. Iwata**, None

The publication costs of this article were defrayed in part by page charge payment. This article must therefore be marked "*advertisement*" in accordance with 18 U.S.C. §1734 solely to indicate this fact.

Corresponding author: Takeshi Iwata, National Institute of Sensory Organs, National Hospital Organization Tokyo Medical Center, 2-5-1 Higashigaoka, Meguro-ku, Tokyo 152-8902 Japan; iwatatakeshi@kankakuki.go.jp.

The inherited macular dystrophies comprise a heterogeneous group of blinding disorders characterized by central visual loss and atrophy of the macula and underlying retinal pigment epithelium (RPE).[1] The complexity of the molecular basis of monogenic macular disease is being elucidated through identification of many of the disease-causing genes.[2–8] Because of limitations associated with studies in humans, nonhuman species with phenotypes similar to human macular degeneration have been used as model systems to study these diseases. Rodent models generated by altering the genes homologous to the disease-causing genes in humans are most extensively used in such studies; however, rodents do not have a defined macula and, hence, the clinical symptoms observed in humans with macular degeneration cannot be fully replicated.[9–11] Because the macula is found only in primates and birds, a monkey model of macular degeneration would be extremely valuable for studies elucidating the mechanism and etiology underlying these diseases. A primate model for macular degeneration is much needed to develop sensitive diagnostic techniques and potential therapeutic strategies to cure or prevent the disease. Furthermore, such models are of particular value if their genetic basis is understood.

Macular degeneration in monkeys was first described by Stafford in 1974.[12] He reported that 31 (6.6%) of eyes of elderly monkeys showed pigmentary disorders and/or drusen-like spots. In 1978, El-Mofty et al.[13] reported a high incidence (50%) of maculopathy in a closed rhesus monkey colony at the

Caribbean Primate Research Center of the University of Puerto Rico. The latest report from the center states that specific maternal lineages have a statistically significant higher prevalence of drusen.[14] Although they suspected the involvement of hereditary factors, genetic analysis of the macaque population has not been reported.

We have reported a high incidence of macular degeneration in one of the cynomolgus monkey (*Macaca fascicularis*) colonies at the Tsukuba Primate Center.[15,16] This macular degeneration originated from one affected male monkey, which showed phenotypic characterization of macular degeneration. The disease affects the central retina specifically, with yellowish white dots in the macula and lipofuscin deposits in the RPE, consistent with the phenotype observed in the early stages of age-related macular degeneration (AMD). These symptoms appear at the age of ~2 years and progress slowly throughout life. Mating experiments have demonstrated that this familial macular degeneration is segregating as an autosomal dominant trait.[17]

AMD is currently considered a multifactorial disorder involving both environmental and genetic factors. Recent studies have substantiated the evidence for AMD as a complex genetic disorder in which one or more genes contribute to an individual's susceptibility to the development of the disease.[18–20] To date, full-genome scan studies have indicated that some regions of the genome harbor AMD-predisposing genes.[21,22] However, most genes associated with susceptibility to AMD have not been identified, presumably because of a complex pattern of inheritance, late age of onset, and difficulties in obtaining large pedigrees for standard linkage analysis. Genes implicated in monogenic macular dystrophies that occur earlier in life with a clear pattern of inheritance have been considered as good candidates for susceptibility to AMD.[23–26] To date, 15 macular degeneration genes have been linked or cloned for human macular degeneration (RetNet; http://www.sph.uth.tmc.edu/Retnet/home.htm; provided in the public domain by University of Texas Houston Health Science Center, Houston, TX). However, with the exception of *ABCA4*, none of these genes has shown a convincing association with AMD.

Because the monkey macular degeneration model we present here shares phenotypic similarities with the early stages of AMD, the identification of the gene involved in this monkey pedigree may provide critical clues to the understanding of the mechanism of AMD. In this study, monkey orthologues of the human genes responsible for Stargardt macular degeneration 1 (*ABCA4*),[2] Best macular degeneration (*VMD2*),[3,7] Doyn honeycomb dystrophy (*EFEMP1*),[4] Sorsby fundus dystrophy (*TIMP3*),[5] and Stargardt macular degeneration 3 (*ELOVL4*)[6,8] were cloned and screened for mutations in the affected monkeys. Subsequently, 13 human macular degeneration loci, including these five genes, were analyzed to test for linkage with the disease in the pedigree. During this process, we evaluated the nature and utility of human microsatellite markers in the cynomolgus monkey for linkage studies. This article also describes the gene structure and evolutionary conservation of the five human macular degeneration genes in the cynomolgus monkey.

Materials and Methods

Maintenance of Monkeys

The cynomolgus monkeys in the pedigree with macular degeneration were reared at the Tsukuba Primate Center for Medical Science (National Institute of Infectious Diseases; Tokyo, Japan). All monkeys were treated in accordance with the rules for care and management of animals at the Tsukuba Primate Center[27] under the Guiding Principles for Animal Experiments using Non-Human Primates formulated and enforced by the Primate Society of Japan (1986). All experimental procedures were approved by the Animal Welfare and Animal Care Committee of the National Institute of Infectious Diseases of Japan. These animal protocols fulfill the guidelines in the ARVO Statement for the Use of Animals in Ophthalmic and Vision Research.

Clinical Studies

Fundus photographs, fluorescein angiography (FA), and indocyanine green angiography (IA) were performed with a fundus camera (TRC50; Topcon, Tokyo, Japan) in animals under anesthesia. Electroretinography (ERG) was recorded in four affected and six normal monkeys with a white/color LED stimulator and contact lens electrode (LS-W; Mayo, Aichi, Japan). After 20 minutes of dark adaptation, rod ERG, combined ERG, and oscillatory responses were recorded, and single-flash cone response and 30-Hz flicker ERG were recorded after 10 minutes of light adaptation. The stimulus and recording conditions conformed to the standards for clinical electroretinography recommended by the International Society for Clinical Electrophysiology of Vision.[28]

Genomic DNA and RNA Isolation

Peripheral blood was collected from 19 affected and 11 unaffected monkeys from the pedigree (Fig. 1, asterisks, pound signs) and an

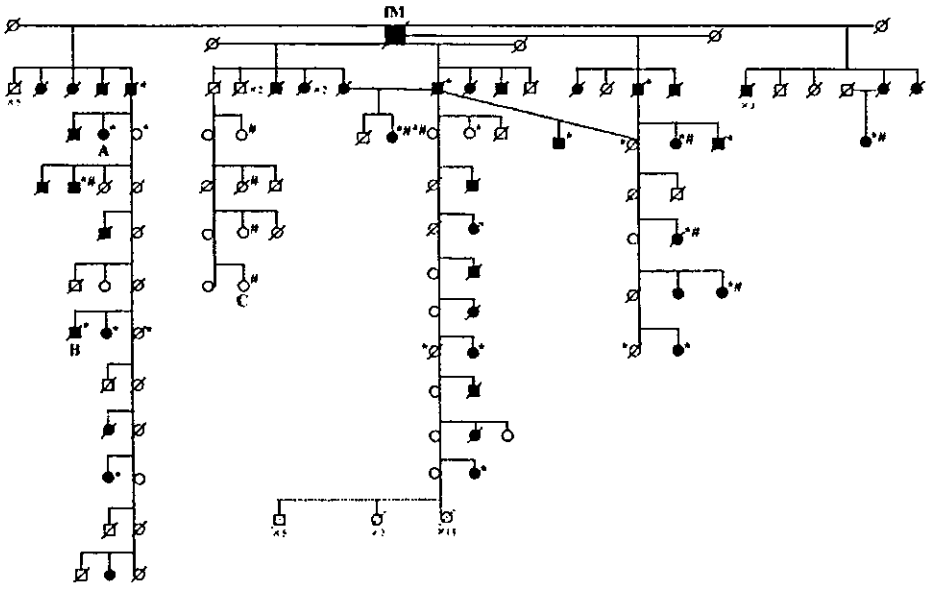

FIGURE 1. Edited version of the monkey pedigree with macular degeneration: fM, the founder breeding male monkey with typical macular degeneration, is shown with five healthy mates arrayed horizontally. The first-generation offspring are also arrayed horizontally. The breeding members from each branch of the first generation offspring are arrayed vertically with their mates and progeny. Monkeys used for *linkage analysis and #mutation screening are marked.

TABLE 1. Primer Sets Used for Cloning of the Monkey Homologues

Gene	Amplified Region	Name	Forward Primer	Position	Name	Reverse Primer	Position	Size (kb)
VMD2	Exon 1	P1F	GACCAGAAACCAGGACTGTTGA	Intron	P1R	GAACTCGCCATATAGCAGCTT	Exon 2	2.1
	Exon 2	P2F	GCTCTGACCAGGGTCTCTGA	Intron	P3R	CCGCACCTTTCCCTGAACTA	Intron	4.5
	Exon 3	P3F	CTAGACCTGGGGACAGTCTCA	Intron	P3R	CCGCACCTTTCCCTGAACTA	Intron	0.3
	Exon 4-5	P4F	CACGGAAGAACAACAGCTGA	Exon 3	P5R	ACACCAGTGGGATACTAATCCAG	Exon 6	2.3
	Exon 6	P6F	GCCAGGAATGGACCATGAGTA	Intron	P6R	GAGCCACTTAGCCTCTAGGTGA	Intron	0.3
	Exon 7-8	P7F	CCTGGAGCATCCTGATTTCA	Intron	P8R	TGAGGCCTCCCTACAGAACA	Intron	2.3
	Exon 9	P9F	TGGCAGAGCAGCTCATCA	Exon 8	P9R	AGCTTCCAGGCCTTGTTG	Exon 10	3.0
	Exon 10	P10F	AAGGGAGAAGGCCAGGTGTT	Intron	P10R	TTTCCTGTAGTGCTTGGGTACTA	Intron	1.2
	Exon 11	P11F	TGCCCTCCTACTGCAACATT	Intron	P11R	ATGCAATGGAGTGTGCATTA	Intron	1.1
EFEMP1	Exon 1	P1F	TTCTAGAACCCTCTGGTCTCTGA	Intron	P1R	CCCTTTCTTAACAGCAAGCTAAC	Intron	0.9
	Exon 2	P2F	GATTGGAAGTTGAGTATGGTGGA	Intron	P2R	CATTCTAGGGATAATGTGGTACCAA	Intron	1.3
	Exon 3-4	P3F	AAGATGGTACTGGGCAACTGTAC	Intron	P4R	ACATCTGTAGAGTAGCTTGACAGCA	Intron	1.4
	Exon 5	P5F	CTACACAGGCTAGAGGAATATGATCA	Intron	P5R	GACACAGGATTTAAGTAACTTGCTCA	Intron	1.3
	Exon 6-7	P6F	CACTGAATGGCATGAACATTG	Intron	P7R	TAGAACAGAATTCCCATGGGTAA	Intron	1.6
	Exon 8	P8F	AATAGGACAAGAAGCCAGATCTCT	Intron	P8R	TTCCTGGTTAAAACTAAATACCTAACA	Intron	0.4
	Exon 9-10	P9F	AACAGATGAACAATAGGTGCTTGA	Intron	P10R	TATCTATCTGGCAGTGTTACCAAGA	Intron	0.9
	Exon 11	P11F	GTATTAGACAAGGGATAAGAGCCAA	Intron	P11R	CAGAGGTTATGCATATATGCTGTGA	Intron	1.7
TIMP3	Exon 1	P1F	CCCAGCGGTATATCACTCG	Intron	P1R	AGCCACTGTGAGTTTCCTCTG	Intron	0.7
	Exon 2	P2F	CAATGGCTCTAACAGGAGAAGTAG	Intron	P2R	CTTGACCAAGGTCTCATGGTTA	Intron	0.8
	Exon 3-4	P3F	TCCAGTTCCAGCTGCATTG	Intron	P4R	AGTTAGTGTCCAAGGGAAGCT	Exon 5	2.6
	Exon 5	P5F	ATGTACCGAGGCTTCACCAA	Exon 3	P5R	AGGTGAGCTAAACACTATTCTGGA	Intron	3.5

additional six unrelated normal monkeys, and genomic DNA was extracted (QIAamp DNA Blood Maxi Kit; Qiagen, Valencia, CA). A normal monkey outside the pedigree was killed for bilateral eye enucleation, and enucleated eyes were immersed and stored in RNA-stabilization solution (RNAlater; Ambion, Austin, TX) at −80°C until RNA isolation. After thawing on ice, the eyeballs were dissected to separate the neural retina and choroid followed by extraction of total RNA.

Histologic Studies

An affected 14-year-old male monkey (Fig. 1, monkey B) was killed for histologic studies. Enucleated eyes were fixed in 10% neutralized formaldehyde solution at 4°C overnight, dehydrated, and embedded in paraffin. Four-micrometer-thick sections were prepared and stained with hematoxylin and eosin (HE) or periodic acid–Schiff (PAS). Serial sections were used for immunohistochemical analysis with anti-complement 5 (C5) antibody. After pretreatment with 0.4 mg/mL proteinase K in phosphate-buffered saline (PBS) for 5 minutes and blocking with 5% skim milk in PBS for 20 minutes at room temperature, the sections were incubated with rabbit anti-human C5 polyclonal antibody (Dako, Glostrup, Denmark) diluted to 1:200 dilution in PBS for 2 hours at room temperature. Alexa 488–conjugated goat anti-rabbit IgG (Molecular Probes, Eugene, OR), diluted to 1:200 in PBS, was used as the secondary antibody. The negative control experiments were performed using normal rabbit immunoglobulin fraction (Dako) instead of anti-C5 antibody.

Characterization of the Genomic Organization and cDNA Sequence of the Monkey *ABCA4*, *VMD2*, *EFEMP1*, and *TIMP3* Genes

Gene-specific primers of the human macular degeneration genes *ABCA4*, *VMD2*, *EFEMP1*, and *TIMP3* were designed based on the human genomic DNA sequence to amplify exons of monkey genes (Table 1). Amplified products were directly sequenced. For all genes except *ABCA4*, the 5′/3′-rapid amplification of cDNA ends (5′/3′-RACE) was performed using total RNA isolated from the monkey retina. Amplification of partial cDNAs by both 5′- and 3′-RACE was designed to generate overlapping PCR products to obtain a full-length cDNA sequence. Primers were initially designed based on the exonic sequences obtained by genomic sequence (Table 2). RACE products were subcloned into the pCRII cloning vector (TA Cloning Kit Dual Promoter; Invitrogen, Carlsbad, CA) and sequenced directly. The obtained nucleotide sequence data have been submitted to GenBank, and assigned accession numbers: *TIMP3*: AY207381-207385, AH012631; *EFEMP1*: AY312407-312415, AH012997; *VMD2*: AY357925-357936, AH013172; *ELOVL4*: AF461182-461187, AH012403; *ABCA4*; AY793687 (http://www.ncbi.nlm.nih.gov/Genbank; provided in the public domain by the National Center for Biotechnology Information, Bethesda, MD).

Mutation Analysis

Coding regions and adjacent intronic sequences of the monkey *ABCA4*, *VMD2*, *EFEMP1*, *TIMP3*, and *ELOVL4* genes were analyzed for sequence variants by single-strand conformation polymorphism (SSCP) or denaturing (D)HPLC (for the *ABCA4* gene) analysis in parallel with direct sequencing. Genomic DNA from six affected and five unaffected monkeys from the pedigree (Fig. 1, pound signs) and six unrelated normal subjects were used for mutation analysis. Primers located in the intronic regions were designed to amplify coding sequences of individual genes (Table 3). Large exons were divided into smaller segments to obtain amplification products suitable for SSCP analysis. The purified amplicons were analyzed by SSCP or DHPLC analysis, as previously described.[29,30] All the samples were also analyzed by bidirectional sequencing with the PCR primers. Exons 2, 7, and 10 of the *VMD2* gene were screened for sequence variants only by direct sequencing.

TABLE 2. Primers for 5′-3′-RACE

Gene	5′-RACE	Position	3′-RACE	Position
VMD2	GTATACACCAGTGGGATA	Exon 6	AGAGCAACAGCTGATGTTTGAGAA	Exon 3
EFEMP1	GGATGGTACATTCATCTA	Exon 7	GATCCTGTGAGACAGCAATGCA	Exon 3
TIMP3	ATCATCTGGGAAGAGTTA	Exon 5	GATGAAGATGTACCGAGGCTTCA	Exon 2-3

TABLE 3. Primer Sets Used for Mutation Screening

Gene	Exon No.	Length (bp)	Name	Forward Primer	Name	Reverse Primer	Size (bp)
ABCA4	1	66	01F	TCTTCGTGTGGTCATTAGC	01R	ACCCCACACTTCCAACCTG	152
	2	91	02F	AAGTCCTACTGCACACATGG	02R	CTAGACAAAAGGCCCAGACC	266
	3	142	03F	TTCCCAAAAAGGCCAACTC	03R	CACGCACGTGTGCATTTCAG	301
	4	139	04F	GCTATTTCCTTATTAATGAGGC	04R	GGGAAATGATGCTTGAGAGC	212
	5	128	05F	CCCTTCAACACCCTGTTCTT	05R	TTCTTGCCTTTCTCAGGCTGG	237
	6	198	06F	GTATTCCCAGGTTCTGTGG	06R	TACCCCAGGAATCACCTTG	330
	7	88	07F	AGCATATAGGAGATCAGACTG	07R	GGCATAAGAGGGGTAAATGG	241
	8	238	08F	GAGCATTGGCCTCACAGCAG	08R	CCCCAGGTTTGGTTTCACC	397
	9	139	09F	AGACATGTGATGTGGATACAC	09R	GTGGGAGGTCCAGGGTACAC	271
	10	117	10F	AACACTAAGTGATAGGGGCAGAA	10R	GGCCTGCTTGTTGTATTTTGAT	344
	11	198	11F	AGCTCACTCGCTCTTTAGGG	11R	TTCAAGACCACTTGACTTGC	406
	12	206	12F	TGGGACAGCAGCCCTTATC	12R	CCAAATGTAATTTCCCACTGAC	362
	13	177	13F	AATGAGTTCCGAGTCACCCTG	13R	CCCATTAGCGTGTCATGG	308
	14	223	14F	TCCATCTGGGCTTTGTTCTC	14R	AATCCAGGCACATGAACAGG	407
	15	222	15F	AGACAGTAACTAACAGGCTCGTG	15R	GGACTGCTACAGACCCTTCC	386
	16	205	16F	CTGTTGCATTGGATAAAAGGC	16R	GATGAATGGAGAGGGCTGG	330
	17	65	17F	CTGCGGTAAGGTAGGATAGGG	17R	CACACCGTTTACATAGAGGGC	232
	18	90	18F	CAGCTCCCGGTGGTAGAGTA	18R	CCCTTGCCATGAGATGTTTT	222
	19	175	19F	TGGGGCCATGTAATTAGGC	19R	TGGGAAAGAGTAGACAGCCG	322
	20	132	20F	GCATGTTGCTAAAGGCCATC	20R	TATCTCTGCCTGTGCCCAG	293
	21	140	21F	GTAAGATCAGCTGCTGGAAG	21R	GAAGCTCTCCTGCTCCAAGC	301
	22	138	22F	CCCTCCACAGTCCCTTAACTC	22R	GAGAGTGGGGACCACAGGTA	244
	23	194	23F	TTTTGCAACTATGTAGCCAGGA	23R	AGCCTGTGTGAGTAGCCATG	384
	24	85	24F	GCATCAGGGAGAGGCTGTC	24R	CCCAGCAATATTGGGAGATG	212
	25	206	IVS24F	GTAAGGACTGGACGGGCCATACTTGG	IVS24R	TCCAGCTCTCTGAAAAGGCTGGCATA	2 kb
			IVS25F	AAAGCTGGTGGAGTGCATTGGTCAAG	IVS25R	CCTGAATCAGAATCCTCCGTGACGTTC	500
	26	49	26F	TCCCATTATGAAGCAATACC	26R	ACCCAGCCCCTTAGACTTTC	228
	27	266	IVS26F	GGATTCTGATTCAGGACCTCTGTTTGC	IVS26R	CTGCGGATGGTGTGTTGGAATCTCTT	2 kb
			IVS27F	TCCCAGAGAGAAGGCTGGACAGACAC	IVS27R	CCCATATATCCAGGGGTGAAGGGTCA	1 kb
	28	125	28F	TGCACGCGCACGTGTGAC	28R	TGAAGGTCCCAGTGAAGTGGG	291
	29	99	29F	CAGCAGCTATCCAGTAAAGG	29R	AACGCCTGCCATCTTGAAC	263
	30	187	30F	GTTGGGCACAATTTCTTATGC	30R	ACTCAGGAGATACCAGGGAC	347
	31	95	IVS30F	GAGAAGCTCACCATGCTGCCAGAGT	IVS30R	GAGATGTTCCTGTCCGTCAGGTCTTG	2 kb
			IVS31F	CGCAGCACGGAAATTCTACAAGACCT	IVS31R	CCTCTGTTCATTGACGCAGAATTTGCT	700
	32	33	32F	ACGGCACTGCTGTACTTGTG	32R	TCAACATGGCTGTGAGGTGT	182
	33	106	IVS32F	GAGCAAATTCTGGGTCAATGAACAGAGG	IVS32R	CGCTTAAAAACCCAACAAGTGCTTCC	1.2 kb
			IVS33F	AGGTATGGAGGAATTTCCATTGGAGGA	IVS33R	CTTTAGAGGCCTCTCTAGTGATAGG	300
	34	75	34F	AAACCGTCTTGTTTGTTTGTTT	34R	AGGAGGGAGGGAATTCAATG	208
	35	170	IVS34F	GGCCCTATCACTAGAGAGGCCTCTAAAG	IVS34R	GGTTGGCTAATGACGGTGATTCCATAC	550
			IVS35F	CATGCCCTGGTCAGCTTTCTCAATGT	IVS35R	GAGAAAATCACGCAGATGGCAACCAC	2 kb
	36	178	36F	TGTAAGGCCTTCCCAAAGC	36R	TGGTCCTTCAGAGCACACAC	346
	37	116	37F	CATTTTGCAGAGCTGGCAGC	37R	CTTCTGTCAGGAGATGATCC	260
	38	158	38F	GGAGTGCATTATATCCAGACG	38R	CCTGGCTCTGCTTGACCAAC	302
	39	125	39F	TGCTGTCCTGTGAGAGCATC	39R	CTTCCAGCCCAACAAGGTC	344
	40	130	IVS39F	CTGCTCATTGTCTTCCCCCACTTCTG	IVS39R	CAGCAGGGTCAGGAGGAAGTACACCA	700
			IVS40F	GTGAGGAGCACTCTGCAAATCCGTTC	IVS40R	AGATGAGGAAAAGGGGTCAGGATTGG	3.5 kb
	41	121	41F	GAAGAGAGGTCCCATGGAAAGG	41R	GCTTGCATAAGCATATCAATTG	299
	42	63	42F	CTCCTAAACCATCCTTTGCTC	42R	AGGCAGGCACAAGAGCTG	214
	43	107	43F	GGTCTCTAGGGGCAGGCTA	43R	CACATCTTTCAGGGCCTCAG	271
	44	142	44F	GAAGCTTCTCCAGCCCTAGC	44R	TGCACTCTCATGAAACAGGC	277
	45	135	IVS44F	ACATCTTTACCTTTATGCCCGGCTTCG	IVS44R	AATGAGTGCGATGGCTGTGGAGAGTT	4 kb
			IVS45F	TTAAGAGCCTGGGCCTGACTGTCTACG	IVS45R	GAATCTCTTGCCTGTGGGATGTGAGG	1 kb
	46	104	48F	GAAGCAGTAATCAGAAGGGC	46R	GCCTCACATTCTTCCATGCTG	257
	47	93	47F	TCACATCCCACAGGCAAGAG	47R	TTCCAAGTGTCAATGGAGAAC	258
	48	250	48F	ATTACCTTAGGCCCAACCAC	48R	ACACTGGGTGTTCTGGACC	365
	49	87	49F	GGTGTAGGGTGGTGTTTTCC	49R	ACTGCCTCAAGCTGTGGACT	187
VMD2	2*	152	P2F	GCTCTGACCAGGGTCTCTGA	P3R	CCGCACCTTTCCCTGAACTA	4.5 kb
	3	95	P3F	CTAGACCTGGGGACAGTCTCA	P3R	CCGCACCTTTCCCTGAACTA	325
	4	234	MP4aF	TGGGAGACAGAACCCTTGGA	MP4aF	GTCCTTGCCTTCCACGAA	302
			MP4bF	TGGTGGAACCAGTACGAGAA	MP4bF	TCCACCCATCTTCCATTGTT	286
	5	155	MP5F	AAAGGAGTGCTGAGGTTCCTATA	MP5R	CTTGTTTCCTGTGAACCACAA	330
	6	78	P6F	GCCAGGAATGGACCATGAGTA	P6R	GAGCCACTTAGCCTCTAGGTGA	292
	7*	153	P7F	CCTGGAGCATCCTGATTTCA	P8R	TGAGGCCTCCCTACAGAACA	2.3 kb
	8	81	MP8F	GCATCATGTGGTGTGGAAAT	P8R	TGAGGCCTCCCTACAGAACA	270
	9	152	MP9F	CAAGTCATCAGGCACGTACAA	MP9R	CTAGGCAGACCCCTGCTACTA	286
	10*	639	P10F	AAGGGAGAAGGCCAGGTGTT	P10R	TTTCCTGTAGTGCTTGGGTACTA	1.2 kb
	11	19	P11F	TGCCCTCCTACTGCAACATT	MP11R	AAGTAGTCCTGGACTGCTGATTT	270
EFEMP1	2	81	MP2F	CCGCAGCAGATACTAAATATCAG	MP2R	CCGCTGAACCGTACTTATTTC	173
	3	49	MP3F	CTTAGGGAATGGACACACCAA	MP3R	ACAGAAGGCCAAAGATCACAT	155

(continues)

TABLE 3. (*continued*).

Gene	Exon No.	Length (bp)	Name	Forward Primer	Name	Reverse Primer	Size (bp)
	4	387	MP4aF	CCCTCTTAGAAGATTCCTGACTTA	MP4aR	ACACTCCACTGGTTGCCAT	249
			MP4bF	ATGAACAGCCTCAGCAGGA	MP4bR	GCAAAAGCTTTCGATGGTTA	316
	5	123	MP5F	GGAGGCAATATCAACATCTTCA	MP5R	TGCTTGAGGTTGAAACAGTTAAG	248
	6	120	MP6F	GCAAACAGCAATGCTAATTCA	MP6R	GAAATACTGCAACATGGCATG	250
	7	120	MP7F	CAGCTAGGGAATTATTTATCAGCA	MP7R	CAGGGATTGGACTTTATTCCA	279
	8	120	MP8F	ATATCCAAAGTAGTGGTGCACAA	P8R	TTCCTGGTTAAAACTAAATACCTAACA	235
	9	124	MP9F	TGCAAACAGAATCTGCCAGTA	MP9R	TTTGGCTTGGTAAGACCAGAA	265
	10	196	MP10F	CTTACCAAGCCAAACTGCTAACTA	MP10R	AACAAACTCCCATCTTTCTCAATAG	289
	11	162	MP11F	AAAGCATAGAAAGTCCAATGCA	MP11R	AGGTAACAATATTCTTTGGCTGACT	281
ELOVL4	1	100	MP1F	CCGCGGTTAGAGGTGTTC	MP1R	GAGACCAGGGGTCGGTGAC	281
	2	188	MP2aF	TTGAGACATCTTGATTCCTAGAAAG	MP2aR	AAGTTAAGCAAAACCATCCCA	252
			MP2bF	CTGGGTCCAAAGTGGATGAA	MP2bR	AGCTAACAGTTATGTCTGGGTACAA	213
	3	81	MP3F	GCAATTGGAATGCATGACA	MP3R	TTTCACAGATTGGGGCCTATA	304
	4	172	MP4aF	AAATGATTCCATGCCTTGTACA	MP4aR	AACGCAAGCAGTATATTCCTGA	330
			MP4b	TGGTGTTTATAACACGCTTTCC	MP4bR	CTCATTGCTTTCCACTGAACA	271
	5	128	MP5F	ATCTCGGTGGCTTACTGCTTA	MP5R	AATAAGTCGGCTGGAGTCAACT	356
	6	276	MP6aF	TTGGGCCTGTGATAGCTATG	MP6aR	TTAGGCTCTTTGTATGTCCGAA	247
			MP6bF	CTCTAATTGCCTAGGCAATCAG	MP6bR	GGGAGTTTTTCCTCACTGTCA	242
TIMP3	1	121	MP1F	AACTTTGGAGAGGCGAGCA	MP1R	CCTAAGCAGCGCTGCAGTC	233
	2	83	MP2F	TGAGATGCTGTTCCTGATGTG	MP2R	GGCTGGTGCTTAGACACACA	266
	3	112	MP3F	AGCAGTGGGATTATGGATCATAC	MP3R	ACATTTGGTGAGTCAGCTACTCA	267
	4	122	MP4F	TGGGCTAAGTGGGAACATAGTA	MP4R	GTTTCTAGGGCTGCAAGTCA	274
	5	198	MP5F	TACCATGGCAGATTCCATCA	MP5R	AGTTAGTGTCCGAGGGAAGCT	306

* Exon 2, 7, and 10 of the *VMD2* gene were screened for sequence variants only by direct sequencing.

Linkage Analysis

Linkage analysis was performed on DNA from 19 affected and 7 unaffected members of the pedigree. Individuals used for the analysis are indicated by asterisks in Figure 1. Human microsatellite markers linked to human macular degeneration loci were analyzed with monkey genomic DNA used as the template. Details of microsatellite markers and their primer sequences were obtained from the genome database. Microsatellite marker analysis was performed by two methods: Markers linked to candidate gene loci and included in a linkage mapping set (ver. 2.5MD10; Applied Biosystems, Inc. [ABI], Foster City, CA) were analyzed on the a DNA sequencer (model 3100; ABI) with fluorescence-labeled primers. Additional microsatellite markers were analyzed by ^{32}P dCTP incorporation into the amplified product.[51] Two-point linkage analysis was performed between the disease locus and microsatellite markers with the MLINK program of the LINKAGE package, as described elsewhere.[52,53] Linkage was assessed under the conditions of autosomal dominant inheritance of the disease trait with a frequency of 0.001 for the disease-causing allele, by using the affecteds-only model, as published earlier.[51] Linkage analysis was performed assuming equal frequencies for marker alleles. Haplotypes were constructed with genotypes of microsatellite markers according to their order on human chromosomes.

RESULTS

Clinical and Histologic Findings

Fundus photographs and FA of a 14-year-old female affected monkey (Fig. 1, monkey A) are shown in Figure 2. Fine, yellowish white dots were observed in the maculae (Figs. 2a–d), scattered in the peripheral retina along blood vessels in this monkey (Figs. 2a, 2b). However, in most cases, the locations of the lesions fell within the region centered on the fovea centralis with the same diameter as one optic disc. FA showed hyperfluorescence corresponding to these dots, except foveola (Figs. 2e, 2f). No abnormalities were found in the optic disc, retinal blood vessels, or choroidal vasculatures in any eyes examined. The amplitude and peak latency of both dark- and light-adapted ERG showed no alteration compared with normal control eyes, indicating that global rod or cone degeneration was absent. Histologic studies demonstrated that there were various-sized drusen, weakly stained by PAS (light purple), between the RPE and choriocapillaris in the macular region (Figs. 3a, 3b, asterisk). These drusen were strongly reactive with antibodies against complement C5 (Figs. 3c, 3d). This finding was consistent with the property of drusen reported in patients with AMD.[35] Accumulation of lipofuscin in RPE cells was also obvious by PAS (Figs. 3a, 3b, deep purple, arrows).

Mutation Analysis of the *ABCA4*, *VMD2*, *EFEMP1*, *TIMP3*, and *ELOVL4* Genes

To evaluate the involvement of the *ABCA4*, *VMD2*, *EFEMP1*, *TIMP3*, and *ELOVL4* genes in disease, we first determined the genomic sequence and the complete cDNA sequence of the orthologous genes in the monkey. Subsequently, these genes were screened for sequence variants in affected and unaffected monkeys in the pedigree, in addition to unrelated, unaffected animals by SSCP, or by DHPLC for the *ABCA4* gene, analysis and direct sequencing.

ABCA4. The monkey *ABCA4* gene consists of 50 exons, with its translation stop codon in exon 50, similar to the human gene. The complete 6819-bp cDNA encodes a protein of 2273 amino acids. *ABCA4* is a member of the superfamily of ATP-binding cassette (ABC) transporters, which are associated with membranes and transport various molecules across extra- and intracellular membranes of all cell types. ABC genes typically encode four domains that include two conserved ATP-binding domains and two domains with multiple transmembrane segments. Comparative sequence analysis revealed that the monkey ABCA4 protein was only 1.8% (41 amino acids) different from the human orthologue, whereas the sequence was identical in the two adenosine triphosphate (ATP)-binding domains. Five of the 41 nonconserved amino acids in the monkey protein (codons 223, 423, 1300, 1817, and 2255) involve polymorphisms in the human. Surprisingly, the Lys223Gln and Arg1300Gln changes reported to be associated with Stargardt disease in humans were observed in the homozygous state in

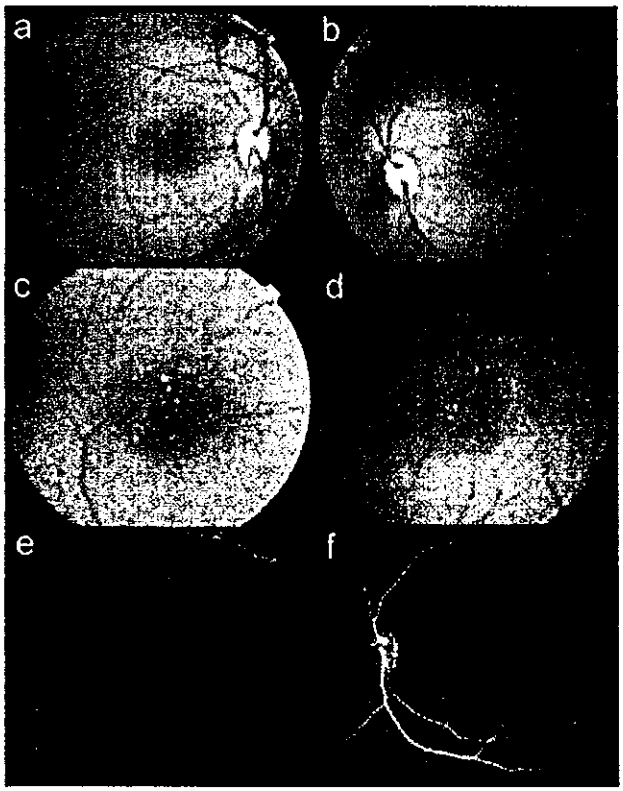

FIGURE 2. Fundus photographs and fluorescein angiogram (FA) of a 14-year-old female cynomolgus monkey (Fig. 1, monkey A) with macular degeneration, showing the right (**a**, **c**, **e**) and left (**b**, **d**, **f**) posterior poles. Fine *grayish white* or *yellowish white* dots were visible in the macula (**a**–**d**). The dots were observed in the peripheral retina along blood vessels in this monkey (**a**, **b**). These dots showed hyperfluorescence in FA except in the foveola (**e**, **f**). High-magnification of the macular region (**c**, **d**, **e**).

one normal control monkey (Fig. 1, monkey C). In addition, the mutation analysis revealed heterozygous amino acid changes at five positions—Leu424Val, Arg1017His, Val1114Ile, Ile1615Val, and Pro2238Gln—in both affected and normal monkeys. However, these missense variants did not segregate with the disease phenotype.

VMD2. The monkey *VMD2* gene consists of 11 exons, with its translation initiation codon in exon 2, as observed in its human orthologue. The complete cDNA was 2187 bp, encoding 585 amino acids. The *VMD2* gene encodes the bestrophin protein, which localizes to the basolateral plasma membrane of the RPE with the postulated function as an oligomeric chloride channel.[36,37] The hydropathy profile predicted that bestrophin contains four stretches of hydrophobic amino acids that function as transmembrane domains. Comparative sequence analysis demonstrated that monkey bestrophin had 19 amino acids different from its human homologue, and the four putative transmembrane domains are highly conserved. To date, 72 disease-associated nucleotide substitutions of the *VMD2* gene have been identified in patients with Best disease.[3,7,26] The mutation analysis of the *VMD2* gene in the monkey pedigree detected six amino acid sequence variants. A polymorphism (Val/Ile) was detected at codon 275 in the fourth transmembrane domain, which has also been reported in humans.[26] Four polymorphisms (Tyr465His, Thr542Met, Glu557Gln, and Thr566Ala) were detected in exon 10. These changes did not segregate with the disease. In addition, one nonsense mutation at codon 582 (Glu→Stop) in exon 11 was detected in two normal monkeys, whereas none of the examined six affected monkeys showed the change.

EFEMP1. The exon–intron gene structure of the monkey *EFEMP1* gene was also similar to the human *EFEMP1* gene. It was composed of 11 exons with its translation initiation codon in exon 2. The complete cDNA was 2034 bp, encoding 493 amino acids. Although the function of this gene remains unclear, this class of proteins is known to have characteristic sequence of repeated calcium-binding EGF-like domains.[4] The monkey *EFEMP1* cDNA was found to have six EGF repeats. Four EGF repeats (numbers 2–5) are encoded by single exons (exons 5–8), one EGF repeat (number 1) is encoded by three exons (exons 2–4), and EGF repeat number 6 is encoded by two exons (exons 9, 10). This finding is in agreement with one of the two transcriptional variants with a distinct 5′ untranslated region (UTR) described in its human homologue. Comparative sequence analysis demonstrated that the monkey *EFEMP1* has three amino acids different from that of the human, but the sequence in the entire region of six EGF repeats is completely conserved. In humans, a single mutation (Arg345Trp) that disrupts one of these domains is known to cause Malattia Leventinese.[4] No amino acid–changing polymorphisms were found in all the monkeys tested. Three single nucleotide polymorphisms (SNPs), that did not alter the amino acid sequence, were detected in exons 4, 5, and 10.

TIMP3. The monkey *TIMP3* gene consisted of five exons, similar to its human orthologue. The complete cDNA was 1887 bp in length, encoding 211 amino acids. *TIMP3* is the third member of the tissue inhibitors of metalloproteinase family, a group of zinc-binding endopeptidases involved in the degradation of the extracellular matrix. *TIMP3* has 12 cysteines characteristic of the TIMP family, which are proposed to form intramolecular disulfide bonds and tertiary structure for the functional properties of the mature protein. The predicted amino acid sequence of the monkey *TIMP3* gene was identical with the human orthologue, including the 12 cysteine residues. Mutations in the *TIMP3* gene are known to cause Sorsby's fundus dystrophy.[5] With a few exceptions,[38,39] most previously described mutations disrupt the disulfide bonds by changing residues into cysteines, leading to misfolding of the protein.[5,40] No coding sequence changes were detected in the *TIMP3* gene in monkeys by mutation screening.

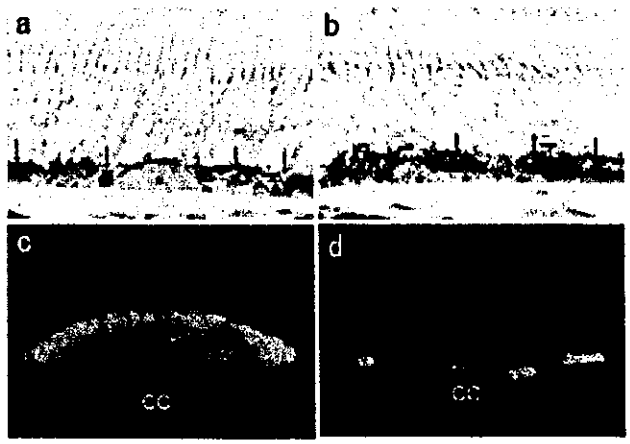

FIGURE 3. Drusen in the affected monkey retina. An affected 14-year-old male monkey (Fig. 1, monkey B). There were various-sized drusen, which were weakly stained by PAS (*), between the RPE and choriocapillaris (CC) (**a**, **b**). These drusen were strongly reactive with antibodies against complement C5 (*green* channel). Lipofuscin autofluorescence is shown (*red*) in the RPE (**c**, **d**). Accumulation of lipofuscin in RPE cells was also obvious by PAS (**a**, **b**, *arrows*).

TABLE 4. Two-Point Lod Scores between the Monkey Macular Degeneration Locus and Markers at the Human Macular Degeneration Loci

Markers	Distance from the Gene (CM)	Order on the Chromosome (M)	Lod Scores at θ									Exclusion ($Z = -2$)
			0	0.001	0.005	0.01	0.05	0.1	0.2	0.3	0.4	
CORD8		154.28										
D1S431	10.5	165	$-\varepsilon$	−2.116	−1.422	−1.128	−0.483	−0.248	−0.071	−0.01	0.006	0.001
D1S2635	0	154.28	$-\varepsilon$	−11.078	−7.598	−6.112	−2.773	−1.469	−0.392	0.019	0.119	0.075
D1S2715	−6.9	147.01	$-\varepsilon$	−7.7	−4.925	−3.747	−1.162	−0.252	0.388	0.464	0.299	0.03
D1S498	−10.6	144.94	$-\varepsilon$	−1.124	−0.439	−0.154	0.416	0.564	0.567	0.433	0.227	0.0001
ABCA4		94.1										
D1S188	−2.3	91.7	$-\varepsilon$	−6.139	−4.058	−3.175	−1.24	−0.541	−0.05	0.074	0.066	0.01
D1S2849	−1.2	92.9	$-\varepsilon$	−1.766	−1.075	−0.784	−0.166	0.032	0.133	0.119	0.067	
D1S2868	0.1	94	$-\varepsilon$	−14.824	−10.623	−8.809	−4.599	−2.846	−1.264	−0.522	−0.146	0.1
STGD3		80.5										
D6S1662	−2.67	77.83	$-\varepsilon$	−1.232	−0.544	−0.257	0.324	0.476	0.472	0.34	0.17	0.0
D6S1048	0.28	80.78	$-\varepsilon$	−0.063	0.614	0.889	1.38	1.416	1.172	0.79	0.362	0.0
D6S1596	7.1	87.6	$-\varepsilon$	−8.746	−5.965	−4.78	−2.138	−1.127	−0.319	−0.025	0.049	0.05
D6S1609	12.08	92.58	$-\varepsilon$	−7.326	−5.235	−4.34	−2.302	−1.475	−0.724	−0.349	0.131	0.05
DHRD		56.1										
D2S2230	3.9	60	$-\varepsilon$	−11.691	−8.209	−6.719	−3.349	−2.006	−0.842	−0.325	−0.084	0.1
D2S378	1.1	57.2	$-\varepsilon$	−9.268	−6.482	−5.29	−2.593	−1.517	−0.588	−0.186	−0.019	0.05
ARMD1		192.2										
D1S384	−2.11	190.09	$-\varepsilon$	−5.565	−3.486	−2.606	−0.696	−0.032	0.375	0.389	0.236	0.01
D1S413	2.1	194.1	$-\varepsilon$	−11.068	−7.59	−6.106	−2.784	−1.501	−0.46	−0.067	0.047	0.05
D1S2622	3.7	195.9	$-\varepsilon$	−1.961	−1.271	−0.982	−0.375	−0.185	−0.084	−0.066	−0.047	0.0
VMD2		61.5										
D11S1993	−2.3	59.2	$-\varepsilon$	−1.615	−0.925	−0.636	−0.032	0.151	0.224	0.181	0.1	0.0
D11S4174	1.4	62.9	$-\varepsilon$	−7.132	−5.026	−4.112	−1.979	−1.102	−0.368	−0.087	0.003	0.01
D11S4076	7.3	66.8	$-\varepsilon$	−5.617	−3.537	−2.656	−0.736	−0.061	0.364	0.385	0.231	0.01
Rhodopsin		130.6										
D3S3515	−4.01	126.59	$-\varepsilon$	−2.756	−1.379	−0.803	0.383	0.717	0.775	0.584	0.302	0.001
D3S3720	−2.8	127.8	$-\varepsilon$	−2.626	−1.247	−0.67	0.531	0.879	0.945	0.729	0.389	0.001
D3S1269	0.3	130.9	$-\varepsilon$	−11.566	−8.081	−6.588	−3.2	−1.846	−0.7	−0.238	−0.062	0.05
Timp3		31.5										
D22S1162	7.05	38.55	$-\varepsilon$	−3.587	−2.203	−1.619	−0.365	0.055	0.291	0.276	0.159	0.005
D22S280	0	31.5	$-\varepsilon$	−4.051	−2.664	−2.075	−0.785	−0.321	−0.002	0.065	0.044	0.01
D22S273	−1	30.5	$-\varepsilon$	−1.878	−1.187	−0.896	−0.278	−0.078	0.026	0.025	0.004	0.0
CTRP5		118.7										
D11S4127	−1.6	117.1	$-\varepsilon$	−0.771	−0.088	0.192	0.73	0.827	0.719	0.495	0.244	0.0
D11S924	0.2	118.9	$-\varepsilon$	−1.424	−0.736	−0.449	0.137	0.298	0.322	0.232	0.113	0.0
D11S4129	4.18	121.58	$-\varepsilon$	−9.057	−6.275	−5.089	−2.435	−1.41	−0.566	−0.214	−0.054	0.05
STGD4		26.1										
D4S403	0	26.1	$-\varepsilon$	−16.798	−11.919	−9.83	−5.081	−3.159	−1.445	−0.633	−0.206	0.1
D4S391	1.2	27.3	$-\varepsilon$	−3.615	−2.231	−1.647	−0.392	0.026	0.255	0.234	0.13	0.005
CORD5	(Interval)	64.5										
D17S938	0	64.5	$-\varepsilon$	−16.296	−11.422	−9.339	−4.638	−2.776	−1.176	−0.466	−0.125	0.1
D17S796	0	64.5	$-\varepsilon$	−3.594	−2.209	−1.624	−0.358	0.075	0.324	0.305	0.176	0.0
MCDR1	(Interval)	98.1										
D6S434	4.3	102.4	$-\varepsilon$	−4.496	−3.103	−2.507	−1.163	−0.632	−0.183	−0.005	0.043	0.0
CORD9	(Interval)	47.6										
D8S1820	0	47.6	$-\varepsilon$	−11.981	−8.501	−7.014	−3.65	−2.277	−1.002	−0.385	−0.092	0.1

ELOVL4. We have reported cloning and characterization of the *ELOVL4* gene in the cynomolgus monkey.[11] Three mutations leading to truncation of the *ELOVL4* protein were reported in humans with Stargardt-like macular dystrophy[23,42] (Karen G, et al. *IOVS* 2004;45:ARVO E-Abstract 1766). Mutation analysis of monkeys with macular degeneration did not detect any amino acid–altering sequence changes. Silent polymorphisms were observed in exons 1, 3, and 4 of the *ELOVL4* gene.

Linkage Analysis of Candidate Gene Loci

The methodology we used to screen for mutations in the candidate genes could miss disease-associated changes that may be present in the promoter or intronic regions; therefore, linkage analysis was performed to exclude the five genes further. Moreover, the macular degeneration phenotype in the monkey pedigree could be caused by a single gene defect. In these cases, linkage analysis would be a comprehensive approach to confirm or exclude a particular gene locus. Microsatellite markers linked to the five candidate gene loci in addition to eight human macular degeneration loci—*ABCA4*, *VMD2*, *DIIRD* (*EFEMP1*), *TIMP3*, *STGD3* (*ELOVL4*), Cone rod dystrophy-8 (*CORD-8*), age-related macular degeneration 1 (*ARMD1*, gene Hemicentin1), rhodopsin, *STGD4*, North Carolina macular degeneration (*MCDR1*), *CORD9*, late-onset retinal degeneration (*CTRP5*), and *CORD5* loci—were analyzed to test for linkage with the macular degeneration in the monkey pedigree. None of the tested loci gave significant positive lod scores (Table 4). We also constructed haplotypes using the genotype data of markers at the 13 loci. This analysis further supported the exclusion of these loci from being among those that might harbor the gene associated with macular degeneration in these monkeys.

Discussion

We report a detailed description of early-onset macular degeneration in cynomolgus monkeys and the exclusion of known genes responsible for macular degeneration in humans as a disease-associated gene in this animal model. Several forms of macular degeneration have been described in humans, including autosomal dominant, autosomal recessive, and X-linked modes of inheritance. The most common form of macular disease in humans is AMD. Major clinical characteristics of AMD are loss of central vision with RPE atrophy or exudation. The presence of subretinal deposits known as drusen is one of the early signs observed in AMD and several other macular degenerations. Recent studies suggest that the process of drusen formation includes inflammatory and immune-mediated events.[35] Immunohistochemical examinations have revealed that drusen contains activated complement factors. These molecules include C5, the cleavage product of C3 (C3b, iC3b, and C3dg), and the terminal complement complex C5b-9. Clinical and histologic studies of the affected monkeys showed the presence of drusen (Figs. 2, 3). Immunologic analysis demonstrated that drusen in monkeys had C5 as a component, suggesting that the nature of monkey drusen was similar to that reported in human AMD. At the same time, the onset of the disease in monkeys is at ~2 years of age; therefore, the monkey macular degeneration resembles early-onset human macular degeneration with drusen.

Comparison of the gene maps and chromosome painting data revealed a high degree of synteny and genome conservation between human and Macaque genomes.[43,44] Amplification of cynomolgus monkey DNA with human microsatellite marker primers and sequence analysis revealed that not only the sequences flanking the microsatellite repeat regions but also the polymorphic nature of these repeats is conserved between human and monkey genomes (data not shown). Comparative studies on human and chimpanzee genomes have shown the same average heterozygosity at microsatellite marker loci and conserved genetic distance between markers.[45] Molecular cloning of monkey orthologues of the human *ABCA4*, *VMD2*, *EFEMP1*, *TIMP3*, and *ELOVL4* genes further demonstrated the high conservation between the human and macaque genomes not only in the organization of the gene structure, but also at the sequence level. Considering the high conservation between human and macaque genomes, human macular degeneration loci can be considered plausible candidates for identification of the gene associated with macular degeneration in the monkeys. We tested this hypothesis using microsatellite markers linked to human macular degeneration loci and successfully amplified microsatellites in the monkey DNA with human primers. However, we failed to establish linkage with the tested loci, and the subsequent haplotype analysis further confirmed this finding. Therefore, the macular degeneration locus in the monkey pedigree is not likely to be associated with the regions of the monkey genome that are syntenic to human genomic regions comprising the 13 macular disease loci tested. Mutation analysis of candidate genes also supported the exclusion of the *ABCA4*, *VMD2*, *EFEMP1*, *TIMP3*, and *ELOVL4* genes. The analyses detected five- and six-amino-acid substitutions in the *ABCA4* and *VMD2* genes, respectively. Some silent nucleotide substitutions or intronic sequences changes, such as small insertions/deletions, SNPs, and variations of short tandem repeats were observed in the *EFEMP1*, *TIMP3*, and *ELOVL4* genes. All these sequence variants did not segregate with the disease phenotype in the extended pedigree. Hence, these changes were interpreted as benign polymorphisms.

In the *ABCA4* sequence of a normal monkey, we found two amino acid replacements (K223Q and R1300Q) that are associated with Stargardt disease in humans. Because of the extensive conservation between the monkey and human gene sequences, one would expect these amino acid changes to have similar disease-associated effects in monkeys. One explanation of this discrepancy could be that K223Q and R1300Q are not causing the disease phenotype in humans, but rather represent markers linked to disease-causing mutations somewhere else in the gene. Alternatively, the disease-causing effect of these amino acid changes on the function of the human ABCA4 protein could be eliminated or compensated for by other differences in the monkey protein. Comparative analysis of the monkey and human genes may provide clues for understanding the molecular pathogenesis caused by *ABCA4* variation. In the *VMD2* gene sequence of normal monkeys, we found a nonsense mutation at codon 582. The change is located at the fourth residue from the C terminus. Bestrophin was shown to form oligomeric chloride channels in cell membranes.[37] The C-terminal cytosolic tail, encoded by exons 10 and 11, has been reported not to be essential for the protein's function. Moreover, although 72 nucleotide substitutions have been identified in Best disease to date,[3,7,26] none of them is reported in exons 10 and 11. Hence, the deletion of four amino acids from the C-terminal end of the protein could be considered not to be associated with the disease.

In summary, we demonstrated that none of the 13 human macular degeneration loci tested were involved in causing the macular degeneration phenotype observed in the monkey pedigree. These results demonstrate the need for additional studies to identify the genetic locus associated with the phenotype in these monkeys and to understand the genetic defect underlying the disease. Identification of the gene responsible for this specific macular degeneration phenotype not only defines a new candidate locus for human macular degeneration, but also provides a primate animal model that can be extensively studied for elucidation of the mechanisms, diagnosis, prophylaxis, and treatment of macular degenerations, including AMD.

References

1. Michaelides M, Hunt DM, Moore AT. The genetics of inherited macular dystrophies. *J Med Genet.* 2003;9:641–650.
2. Allikmets R, Singh N, Sun H, et al. A photoreceptor cell-specific ATP-binding transporter gene (ABCR) is mutated in recessive Stargardt macular dystrophy. *Nat Genet.* 1997;3:236–246.
3. Petrukhin K, Koisti MJ, Bakall B, et al. Identification of the gene responsible for Best macular dystrophy. *Nat Genet.* 1998;3:241–247.
4. Stone EM, Lotery AJ, Munier FL, et al. A single EFEMP1 mutation associated with both Malattia Leventinese and Doyne honeycomb retinal dystrophy. *Nat Genet.* 1999;2:199–202.
5. Weber BH, Vogt G, Pruett RC, Stohr H, Felbor U. Mutations in the tissue inhibitor of metalloproteinases-3 (TIMP3) in patients with Sorsby's fundus dystrophy. *Nat Genet.* 1994;4:352–356.
6. Zhang K, Kniazeva M, Han M, et al. A 5-bp deletion in ELOVL4 is associated with two related forms of autosomal dominant macular dystrophy. *Nat Genet.* 2001;1:89–93.
7. Marquardt A, Stohr H, Passmore LA, et al. Mutations in a novel gene, VMD2, encoding a protein of unknown properties cause juvenile-onset vitelliform macular dystrophy (Best's disease). *Hum Mol Genet.* 1998;9:1517–1525.
8. Bernstein PS, Tammur J, Singh N, et al. Diverse macular dystrophy phenotype caused by a novel complex mutation in the *ELOVL4* gene. *Invest Ophthalmol Vis Sci.* 2001;13:3331–3336.
9. Dithmar S, Curcio CA, Le NA, Brown S, Grossniklaus HE. Ultrastructural changes in Bruch's membrane of apolipoprotein E-deficient mice. *Invest Ophthalmol Vis Sci.* 2000;8:2035–2042.
10. Mata NL, Tzekov RT, Liu X, et al. Delayed dark-adaptation and lipofuscin accumulation in abcr+/− mice: implications for involvement of ABCR in age-related macular degeneration. *Invest Ophthalmol Vis Sci.* 2001;8:1685–1690.

11. Rakoczy PE, Zhang D, Robertson T, et al. Progressive age-related changes similar to age-related macular degeneration in a transgenic mouse model. *Am J Pathol.* 2002;4:1515–1524.
12. Stafford TJ. Maculopathy in an elderly sub-human primate. *Mod Probl Ophthalmol.* 1974;0:214–219.
13. El-Mofty A, Gouras P, Eisner G, Balazs EA. Macular degeneration in rhesus monkey (Macaca mulatta). *Exp Eye Res.* 1978;4:499–502.
14. Hope GM, Dawson WW, Engel HM, et al. A primate model for age related macular drusen. *Br J Ophthalmol.* 1992;1:11–16.
15. Nicolas MG, Fujiki K, Murayama K, et al. Studies on the mechanism of early onset macular degeneration in cynomolgus monkeys. II. Suppression of metallothionein synthesis in the retina in oxidative stress. *Exp Eye Res.* 1996;4:399–408.
16. Nicolas MG, Fujiki K, Murayama K, et al. Studies on the mechanism of early onset macular degeneration in cynomolgus (Macaca fascicularis) monkeys. I. Abnormal concentrations of two proteins in the retina. *Exp Eye Res.* 1996;3:211–219.
17. Suzuki MT, Terao K, Yoshikawa Y. Familial early onset macular degeneration in cynomolgus monkeys (Macaca fascicularis). *Primates.* 2003;3:291–294.
18. Klaver CC, Wolfs RC, Assink JJ, et al. Genetic risk of age-related maculopathy: population-based familial aggregation study. *Arch Ophthalmol.* 1998;12:1646–1651.
19. Seddon JM, Ajani UA, Mitchell BD. Familial aggregation of age-related maculopathy. *Am J Ophthalmol.* 1997;2:199–206.
20. Meyers SM, Greene T, Gutman FA. A twin study of age-related macular degeneration. *Am J Ophthalmol.* 1995;6:757–766.
21. Tuo J, Bojanowski CM, Chan CC. Genetic factors of age-related macular degeneration. *Prog Retin Eye Res.* 2004;2:229–249.
22. Abecasis GR, Yashar BM, Zhao Y, et al. Age-related macular degeneration: a high-resolution genome scan for susceptibility loci in a population enriched for late-stage disease. *Am J Hum Genet.* 2004;3:482–494.
23. Ayyagari R, Zhang K, Hutchinson A, et al. Evaluation of the ELOVL4 gene in patients with age-related macular degeneration. *Ophthalmic Genet.* 2001;4:233–239.
24. Allikmets R. Further evidence for an association of ABCR alleles with age-related macular degeneration: the International ABCR Screening Consortium. *Am J Hum Genet.* 2000;2:487–491.
25. Felbor U, Doepner D, Schneider U, Zrenner E, Weber BH. Evaluation of the gene encoding the tissue inhibitor of metalloproteinases-3 in various maculopathies. *Invest Ophthalmol Vis Sci.* 1997; 6:1054–1059.
26. Lotery AJ, Munier FL, Fishman GA, et al. Allelic variation in the VMD2 gene in best disease and age-related macular degeneration. *Invest Ophthalmol Vis Sci.* 2000;6:1291–1296.
27. Honjo S. The Japanese Tsukuba Primate Center for Medical Science (TPC): an outline. *J Med Primatol.* 1985;2:75–89.
28. Marmor MF, Zrenner E. Standard for clinical electroretinography (1999 update): International Society for Clinical Electrophysiology of Vision. *Doc Ophthalmol.* 1998;2:143–156.
29. Dockhorn-Dworniczak B, Dworniczak B, Brommelkamp L, et al. Non-isotopic detection of single strand conformation polymorphism (PCR-SSCP): a rapid and sensitive technique in diagnosis of phenylketonuria. *Nucleic Acids Res.* 1991;9:2500.
30. Liu W, Smith DI, Rechtzigel KJ, Thibodeau SN, James CD. Denaturing high performance liquid chromatography (DHPLC) used in the detection of germline and somatic mutations. *Nucleic Acids Res.* 1998;6:1396–1400.
31. Griesinger IB, Sieving PA, Ayyagari R. Autosomal dominant macular atrophy at 6q14 excludes CORD7 and MCDR1/PBCRA loci. *Invest Ophthalmol Vis Sci.* 2000;1:248–255.
32. Terwilliger JD, Ott J. *Handbook of Human Genetic Linkage.* Baltimore, MD: The Johns Hopkins University Press; 1994.
33. Otto J. *Analysis of Human Genetic Linkage.* Baltimore, MD: The Johns Hopkins University Press; 1999.
34. Khani SC, Karoukis AJ, Young JE, et al. Late-onset autosomal dominant macular dystrophy with choroidal neovascularization and nonexudative maculopathy associated with mutation in the RDS gene. *Invest Ophthalmol Vis Sci.* 2003;8:3570–3577.
35. Mullins RF, Russell SR, Anderson DH, and Hageman GS. Drusen associated with aging and age-related macular degeneration contain proteins common to extracellular deposits associated with atherosclerosis, elastosis, amyloidosis, and dense deposit disease. *FASEB J.* 2000;7:835–846.
36. Marmorstein AD, Marmorstein LY, Rayborn M, et al. Bestrophin, the product of the Best vitelliform macular dystrophy gene (VMD2), localizes to the basolateral plasma membrane of the retinal pigment epithelium. *Proc Natl Acad Sci USA.* 2000;23: 12758–12763.
37. Sun H, Tsunenari T, Yau KW, Nathans J. The vitelliform macular dystrophy protein defines a new family of chloride channels. *Proc Natl Acad Sci USA.* 2002;6:4008–4013.
38. Tabata Y, Isashiki Y, Kamimura K, Nakao K, Ohba N. A novel splice site mutation in the tissue inhibitor of the metalloproteinases-3 gene in Sorsby's fundus dystrophy with unusual clinical features. *Hum Genet.* 1998;2:179–182.
39. Langton KP, McKie N, Curtis A, et al. A novel tissue inhibitor of metalloproteinases-3 mutation reveals a common molecular phenotype in Sorsby's fundus dystrophy. *J Biol Chem.* 2000;35: 27027–27031.
40. Felbor U, Stohr H, Amann T, Schonherr U, Weber BH. A novel Ser156Cys mutation in the tissue inhibitor of metalloproteinases-3 (TIMP3) in Sorsby's fundus dystrophy with unusual clinical features. *Hum Mol Genet.* 1995;12:2415–2416.
41. Umeda S, Ayyagari R, Suzuki MT, et al. Molecular cloning of ELOVL4 gene from cynomolgus monkey (Macaca fascicularis). *Exp Anim.* 2003;2:129–135.
42. Edwards AO, Donoso LA, Ritter R III. A novel gene for autosomal dominant Stargardt-like macular dystrophy with homology to the SUR4 protein family. *Invest Ophthalmol Vis Sci.* 2001;11:2652–2663.
43. Wienberg J, Stanyon R. Comparative painting of mammalian chromosomes. *Curr Opin Genet Dev.* 1997;6:784–791.
44. O'Brien SJ, Menotti-Raymond M, Murphy WJ, et al. The promise of comparative genomics in mammals. *Science.* 1999;5439:458–462,479–481.
45. Crouau-Roy B, Service S, Slatkin M, Freimer N. A fine-scale comparison of the human and chimpanzee genomes: linkage, linkage disequilibrium and sequence analysis. *Hum Mol Genet.* 1996;8: 1131–1137.

10

次世代サルなどを用いた行動学実験

根岸隆之[a] 川崎勝義[b] 小山高正[c] 黒田洋一郎[d] 吉川泰弘[e]
NEGISHI Takayuki, KAWASAKI Katsuyoshi, KOYAMA Takamasa, KURODA Yoichiro, YOSHIKAWA Yasuhiro
[a]青山学院大学理工学部化学・生命科学科, [b]星薬科大学心理学研究室, [c]日本女子大学人間社会学部心理学科, [d]東京都神経科学総合研究所, CREST, [e]東京大学大学院農学生命科学研究科実験動物学

ヒトの脳の発達障害を研究するためのひとつのツールとして「サル類の行動学実験」を紹介する．ヒト型の実験動物であるサル類は，その行動もヒトと共通する部分が多く，げっ歯類では理解しきれない脳の発達障害による行動異常を評価できる可能性がある．ここで紹介する出会わせ試験，4段指迷路試験，アイコンタクト試験，薬物負荷試験はいずれも簡便であり，神経毒性試験などに広く利用可能と考えられる．

Key words
・サル類
・行動
・社会性
・記憶学習能力
・神経毒性
・実験モデル

はじめに

本稿では，脳機能の発達障害を研究するためのサル類を用いた行動試験法，特にわれわれが開発・改良を続けている試験法を紹介する．近年，脳機能の発達障害に関する研究が重点的に行われるようになり，遺伝子発現レベル，細胞レベル，個体レベルのさまざまな実験から重要な知見が加速度的に集積している．しかし，臨床レベルでの脳の発達障害は，ほぼすべて「行動」が第1の診断基準であることを考えると，「脳の発達障害」を評価・理解するためのエンドポイントもやはり行動と考えるのが妥当である．他方，実験医学分野で最も利用されるげっ歯類(マウス，ラットなど)の行動は，ヒトに外挿しにくい．たとえ遺伝子，細胞，組織レベルはほぼ同一だとしても，行動様式は非常に異なる．そこでわれわれは，ヒト型の実験動物であるサル類を，脳機能の発達障害評価のためのモデル動物として利用することを考えた．これまでにもわれわれは，アルツハイマー病などの加齢性疾患を考えるモデルとして，サル類を対象に *in vitro*・*in vivo* 両面から探ってきた[1)2)]．ここではヒトの行動発達障害を考えるための実験モデルとしてサル類を利用した．

脳の発達障害を評価するためのサル類を用いた行動試験

脳の発達障害(自閉症，学習障害(LD)，注意欠陥多動性障害(ADHD)など)の原因は，今のところ解明されたとは言いがたい．また，遺伝子異常にすべての原因を帰すのも難しい．現在の主流としては，遺伝子・環境の相互作用により胎生期・新生児期の著しいスピードで発達する脳神経系のほんの些細なボタンのかけ違いにより，これらさまざまな脳の発達障害が生じると考えられている．このように未解明

な疾患を研究するアプローチとしては，さまざまなものが考えられる．もちろん遺伝子改変動物が有用であるのは疑いようもなく，コンディショナルノックアウト動物のように時空間特異的に遺伝子発現を操作することも可能であり，分子生物学的に非常に重要な知見をもたらすであろう．一方，われわれが重要な一因と考えているのは，次世代にとっての環境因子(外因性化学物質，母体の異常，出生後の母子行動etc.)であるが，これらの重要性について検討する場合は，その時期(妊娠期・授乳期)に一過性に負荷を与えて生まれてきた個体を遺伝子，細胞，組織，個体とさまざまなレベルで検討するのが一般的である．本稿でいただいたタイトル「次世代サルなどを用いた行動学実験」というのは，脳神経系の発達期・臨界期と考えられている胎生期・新生仔期に何らかの負荷がかかった「次世代サル」に生じるかもしれない，生後，成熟した後も引き続き残存する無処置では修復し得ない不可逆的な障害を評価するための「行動学実験」という意味である．

サル類は昔から，ヒトの精神構造や行動様式を理解するための有用なモデルとして，心理学分野で利用されてきた．その過程で認知，学習記憶などのメカニズムを理解するための多様な行動試験法が開発され，そこで得られた知見が現在のヒト脳の高次機能を理解するための基盤となっていることは疑いない．

脳機能の発達障害を評価するためにも，そのエンドポイントとして行動を選び解析評価することは非常に有意義であるが，心理学的研究が究極の目的とする高次機能そのものの理解と，ここで論じる発達障害の評価を目的とするある意味「障害の有無の可能性」を評価したい場合では，要求される行動実験系が多少異なってくる．というのも，心理学的実験に用いる行動試験は非常に高度な手続きを要求し(だからこそ複雑な機構を理解できるのであるが)，多大な時間と労力を要し，時間および費用の面から多検体を相手にすることが不可能に近い．さらに手続きの複雑さから，実際の試験に用いることのできない個体も少なからず出てくる．それに対して，われわれがここで論じる研究はある意味毒性試験であり，たとえ用いるのがサル類であってもやはり再現性，統計的信頼性という点から多検体を用いた実験を行いたい．可能な限り多くのサル類を試験に処したいと考えると，試験手続きにおいては簡便性(サル類にとっても実験者にとっても)が望まれる．この場合，評価が第一で障害のメカニズムの追求は次の課題となる．われわれは毒性試験においては第一義に要求される，「障害の有無の可能性」をサル類を用いて行動学的に評価するのに適した実験系の開発を行ってきたので，ここではそれらの試験を紹介し，実際に本稿の目的である「脳の発達障害」を評価する試験法としての有用性を論じたい．

出会わせ試験(社会性)

出会わせ試験とは，同世代の2個体を同一ケージに放した際発現する行動を詳細に解析し，攻撃性，相手への興味の程度など，被験動物の社会性を評価する試験である(図1A)．多くの発達障害が社会性の不全を症状のひとつとすることからも，この試験は評価法として有用と考えられる．典型的な次世代を標的とした毒性実験(薬物Aの胎生期曝露など)の場合，複数の群ができるわけであるが，われわれはこの出会わせ試験を同一群内で総当たり戦の形で行う．つまり1群6匹の実験系の場合，計15試験を行う．このやり方は再現性を評価し，統計的信頼性を高める意味で有効であると考えている．被験個体も特に同世代に限定する必要はないが，先に述べたとおり，次世代個体を用いる実験系では必然的に同齢のサル類がそろうことと，あまりに年齢(体格)の離れた2個体では即座に優劣が発生してしまうことから，われわれは同世代による試験を主に行っている．2個体が同一ケージ内で起こす行動をビデオ撮影し，個体識別をしながら複雑な行動を人間の目で解析していくわけであるが，ここで可能な限り客観性を保ちながら詳細に分析できるように，われわれは発生する行動を以前の行動研究[3]を参考に約40項目に設定し，ビデオを5秒間隔で区切り，その5秒間でどの行動が出現したかのみをカウントしてゆく「1/0サンプリン